Ochsner, Christian; Other, Lars; Thiel, Esther; Zuber, Christopher

Working Paper

Demographic aging and long-run economic growth in Germany

Arbeitspapier, No. 02/2024

Provided in Cooperation with:
German Council of Economic Experts

Suggested Citation: Ochsner, Christian; Other, Lars; Thiel, Esther; Zuber, Christopher (2024) : Demographic aging and long-run economic growth in Germany, Arbeitspapier, No. 02/2024, Sachverständigenrat zur Begutachtung der Gesamtwirtschaftlichen Entwicklung, Wiesbaden

This Version is available at:
https://hdl.handle.net/10419/284412

GERMAN COUNCIL
of Economic Experts

Demographic Aging and Long-Run Economic Growth in Germany

Christian Ochsner*)
Lars Other*)
Esther Thiel*)
Christopher Zuber*)

Working Paper 02/2024**)
February 2024

Technical Appendix (PDF)

*) German Council of Economic Experts, E-Mail: christian.ochsner@svr-wirtschaft.de; lars.other@svr-wirtschaft.de; esther.thiel@svr-wirtschaft.de; christopher.zuber@svr-wirtschaft.de

Demographic Aging and Long-Run Economic Growth in Germany*

Christian Ochsner† Lars Other‡

Esther Thiel§ Christopher Zuber¶

German Council of Economic Experts

February 15, 2024

*We thank Tino Berger, Niklas Garnadt, Michael Kogler, Thilo Kroeger, Christian Matthes, Leonard Salzmann as well as Jens Boysen-Hogrefe, Kai Carstensen, Stefan Kooths, Timo Hoffman and other workshop participants the Kiel Institute for the World Economy as well as Rolf Strauch, Konstantinos Theodoridis and other workshop participants at the European Stability Mechanism and participants at the 17th International Conference for Computational and Financial Econometrics for numerous very helpful comments. In addition, we thank Waldemar Hamm, Antonia Koch and Lotte Nacke for research assistance and Michael Schidlowski and the Federal Statistical Office as well as Susanne Wanger and the Institute for Employment Research for immensely valuable help with the data. Finally, we are grateful the council members Veronika Grimm, Ulrike Malmendier, Achim Truger, Monika Schnitzer and Martin Werding for useful discussion. The views expressed here are those of the authors and not necessarily those of the GCEE.

†Email: christian.ochsner@svr-wirtschaft.de; corresponding author.

‡Email: lars.other@svr-wirtschaft.de

§Email: esther.thiel@svr-wirtschaft.de

¶Email: christopher.zuber@svr-wirtschaft.de

Abstract

We study the long-run interaction between Germany's economic growth trajectory and demographic aging. Using a comprehensive dataset, we leverage the classical production function approach to estimate potential output growth between 1970 and 2070. We account for the inherent uncertainty in our projections using Bayesian estimation techniques. Overall, Germany's potential output growth up to 2070 will be low if current economic trends persist. In particular, the diminishing labor volume, coupled with sluggish total factor productivity and investment trend growth, contributes to the decline. Our results highlight the significance of demographic factors in shaping economic trajectories and the critical need for policy interventions to mitigate adverse effects. Our analysis can serve as valuable inputs for formulating long-term economic policies.

Keywords: demographic aging, production function, potential output, Germany, long-run forecast, economic growth

JEL classification: E13, E17, E23

1 Introduction

The economic boom of the post-war period went along with high birth rates in many advanced economies, especially in Europe and Japan, until the 1960s. However, since then, birth rates have declined, and average life expectancy has increased. Consequently, many advanced economies are experiencing rapid aging. For instance, the old age dependency ratio - the proportion of individuals aged over 65 to those aged 20-65 - is projected to significantly change from 26.8 in 2000 to 37.9 in 2023 in Germany, with similar trends observed in France, Italy, Japan, and the United Kingdom. In Germany, demographic aging is expected to be particularly strong in the coming years as the baby boomer generation of the 1950s and 1960s enter retirement age (see Figure 1). This demographic shift poses direct challenges to economic growth, for instance through the reduction in workforce entrants and increase in workforce exits. A growing body of research is now focusing on understanding the economic mechanisms that underlie long-term economic ramifications of demographic aging (see, e.g. Kotschy and Bloom 2023).

Old-age dependency ratio likely to rise sharply in Germany in the next ten years

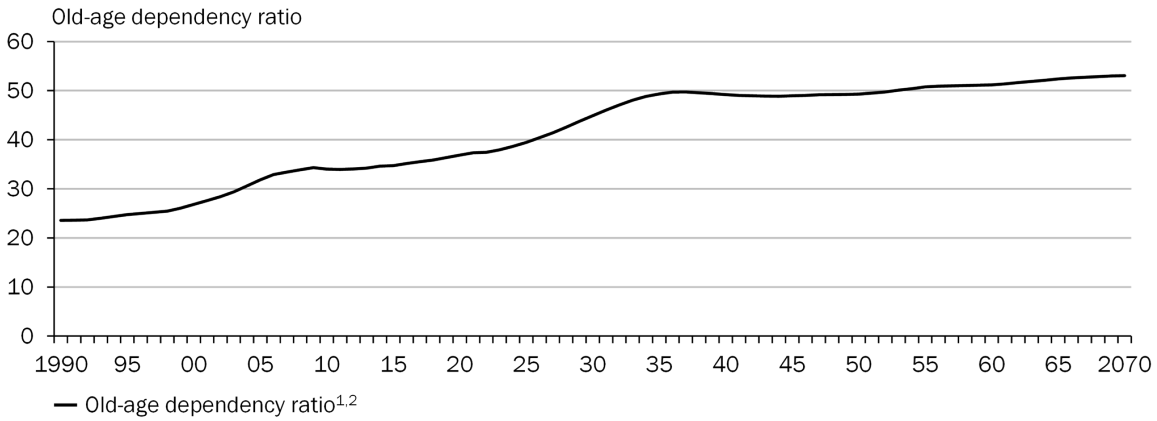

1 – The old-age dependency ratio is the ratio of people aged 65 and older to 100 people aged 20 to 64. 2 – Reference scenario based on the composition of the population in 2022 and assumptions of the medium variant on birth rate (G2), life expectancy (L2) and net migration (W2 with 293,000 persons on average for all years in the projection period) based on the 15th Coordinated Population Projection.

Sources: Federal Statistical Office, Human Mortality Database, SIM.21, own calculations
© Sachverständigenrat | 24-048-01

Figure 1

In this paper, we study the effects of demographic dynamics on the German economy in a two step approach. First, we present a detailed semi-structural growth model in the tradition of production function modelling (Solow 1956, Romer 1986) that enables estimation of potential output since 1970 and explicitly accounts for demographic dynamics. Using this new tool, we forecast potential output in Germany until 2070. Second, counterfactual experiments and micro-data evidence help to rationalise our results, especially with respect to the role of demographic dynamics in Germany's deteriorating economic outlook.

Our growth model features a detailed specification of labor and capital inputs that are

tailored to suit the German economy's characteristics. This allows us to discipline the long-run projections and generate informative, non-mean-reverting dynamics. In particular, to examine the effects of demographic aging on the composition of labor input, the labor participation rate is delineated by an age-cohort model and average hours worked account for deviations between part-time or full-time employees as well as self-employed workers. For capital, we use the perpetual inventory method and account for productivity differences across various types of capital goods weighted by their capital utilization costs (OECD 2009, Knetsch 2013).

Related research emphasizes the role of uncertainty in the very long-run (Müller et al. 2022). While the structure of our growth model is similar to established methods used by institutions like the European Commission and the US Congressional Budget Office for potential output estimation (Havik et al. 2014, Shackleton 2018), we propose substituting the commonly used filter by Hodrick and Prescott (1997) with a Bayesian filtering algorithm. A Bayesian filter can better account for different sources of uncertainty, e.g. parameter uncertainty, that may co-determine long-run results. The associated state-space formulation of our filter gives rise to a natural way of extrapolating the signals into the distant future by means of straightforward, customizable trend-growth specifications.

Our long-term projections of potential output indicate that Germany's growth is expected to slow down due to substantial and continuous demographic changes. More precisely, our results suggest that median growth rates are likely to remain at an average level of approximately 0.4% throughout the 2020s. Without corrective measures, the challenge of slow growth could persist over the next decades. We also identify several factors contributing to the current decrease in Germany's potential growth rates compared to the high levels of around 1,4% per annum seen in the 2010s. While the COVID-19 pandemic and the recent energy crisis may have left scars on the supply side of the economy, the main driver of this adverse trend is the shrinking labor volume as a consequence of an aging German economy. In an auxiliary structural mode, we find that demographic aging affects the labor input of an economy not only through the size of the workforce but also through its composition. This is the case, as young and old cohorts deviate in their labor market characteristics such as participation rate, working hours, and part-time rate. The insights derived from our projections can serve as valuable inputs for long-term economic policy-making and guide actions related to achieving enduring objectives, such as social policy reforms, pension system design or the transition towards a greener economy (Müller et al. 2022).

The paper's structure is as follows: Section 2 outlines the model structure, and Section 3 elaborates on the signal extraction problem. In Section 4, we discuss estimation results. In Section 5, we closely examine the recent deterioration in long-run growth outlook, and Section 6 showcases the model's capabilities for policy evaluation. Section 7 concludes. A set of appendices delve into filtering and estimation algorithms, prior elicitation approaches, model specifications, data, and additional results. Additionally, a Technical Appendix presents detailed estimation and specification results related to total factor productivity, labor volume, and capital services.

2 The Production Function Approach

To evaluate the impact of demographic changes on long-term economic growth, our methodology is anchored in the tradition of macroeconomic theory, as outlined by Solow (1956), Romer (1986), Mankiw et al. (1992), Galor (2011). This tradition emphasizes the essential role of labor, and by extension, demographic factors, in determining the equilibrium output. Here, "equilibrium output" is defined as the level of output attained when input factors are used at its sustainable capacity. Thus, our aim is to model demography as a key determinant of potential output $\overline{y_t}$. This approach of analyzing potential output through production functions, viewed as the economy's equilibrium output trajectory, is well-established. Following this tradition, particularly prevalent in policy-making circles (CBO 1995, Havik et al. 2014, Shackleton 2018, Chalaux and Guillemette 2019, Breuer and Elstner 2020), we estimate the inputs of capital and labor, along with total factor productivity. We then apply a Cobb-Douglas aggregator to compute potential output.

$$\overline{y_t} = \overline{a_t}(\overline{h_t l_t})^{\alpha} \overline{k_t}^{(1-\alpha)}, \tag{1}$$

where $\overline{y_t}$, $\overline{a_t}$, $\overline{h_t}$, $\overline{l_t}$ and $\overline{k_t}$ are the t-th entries in $T \times 1$ vectors of potential output, potential total factor productivity, potential human capital, potential labor and potential capital services. $0 \leq \alpha \leq 1$ is the output elasticity of labor, a known constant. We establish the value of α as 0.66, a choice that closely aligns with the average empirical labor share of gross value added in Germany over the sample period. Note that capital includes tangible as well as intangible assets and that treating human capital as labor-augmenting factor allows to preserve constant returns to scale.

We quantify labor input using total hours worked. To gauge the transmission of demographic aging, we decompose total hours worked into four components as

$$\overline{l_t} = \overline{b_t}\,\overline{w_t}(1 - \overline{u_t})\overline{s_t}, \tag{2}$$

where $\overline{l_t}$ denotes total hours worked, $\overline{b_t}$ represents the working-age population, $\overline{w_t}$ represents aggregate labor participation, $\overline{s_t}$ represents the average number of hours worked per worker, and $\overline{u_t}$ signifies the natural rate of unemployment. This specification enables to examine three possible transmission channels of demographic aging. First of all, the working-age population, determined by birth rates, death rates, and migration patterns, is the key determinant of the potential labor force. Second, the labour force participation represents the proportion of the working-age population (15-74 year olds) actively engaged in the labor market. Demographic aging implies a shift of aggregate labor participation rates to those of older workers (which are typically lower). Finally, the average number of hours worked by individuals in the labor force is influenced by various factors such as part-time, full-time and self-employment rates and hours that are co-determined by worker's age (Wanger 2023).

The equations characterizing aggregate participation as well as average hours worked are

$$\overline{w_t} = \sum_{i=1}^{5} b_{ti} {b_t}^{-1} \overline{w_{ti}} \tag{3}$$

$$s_t = s_t^s q_t^s + (1 - q_t^s)(s_t^p q_t^p + (1 - \overline{q_t^p}) s_t^f) \tag{4}$$

where

- $\overline{w_{ti}}$ and $\overline{b}_{ti}$ denote labor participation of age group i as well as the share of age group i of the working age population,
- $\overline{s_t}^p$ is the number of hours worked by part-time employees
- $\overline{s_t}^s$ is the number of hours worked by self-employed persons
- $\overline{s_t}^f$ is the number of hours worked by full-time employees
- $\overline{q_t}^s$ is the rate of self-employment
- $\overline{q_t}^p$ is the rate of part-time employment
- aggregate labor participation is derived from labor participation in the age groups 15 - 19 year olds, 20 - 59 olds, 60 - 64 year olds, 65-69 year olds, as well as 70 - 74 year olds

In addition, the structural unemployment rate is critical in indicating the equilibrium level of unemployment in an economy. When unemployment falls below the structural unemployment rate, it can exert upward pressure on wages and inflation. Conversely, when unemployment exceeds the structural unemployment rate, it may result in deflationary pressures. To preserve constant returns to scale, we model human capital as a labor-enhancing factor, as shown in Eq. 1. It is given as

$$\overline{h_t} = \exp\{\beta q_t\}. \tag{5}$$

In this equation, β represents the marginal rate of return to education in Germany, which we calibrate to $\beta = 9\%$ in line with studies like Anger et al. (2010) and Pfeiffer and Stichnoth (2021). q is derived from the average number of years of schooling, based on extended data from de la Fuente and Doménech (2006).

To complete the specification of our model, we assess the role of capital in the production process. To this end, we adopt the capital utilization cost approach (OECD 2009, Knetsch 2013). The intuition is to approximate actual capital services by means of weighting gross capital stocks (as a proxy for overall productive capital) of four capital goods, i.e. equipment, residential and non-residential buildings as well as immaterial capital, by their shares in capital utilization costs. The latter approximate the productivity of capital goods. When factors are compensated with their marginal product, higher capital utilization costs imply higher productivity. The year-on-year change in capital services is represented as

$$\dot{\overline{k_t}} = \sum_{j=1}^{4} \dot{v_t}^j \left(\frac{c^j}{c^{j-t}}\right)^{-1}. \tag{6}$$

Here, $\dot{}$ denotes single-period growth rates, ${k_t}^j$ represents capital services, ${v_t}^j$ denotes gross

fixed assets of capital good j, and ${c_t}^j$ is the capital utilization costs of capital good j. We construct the capital services $\overline{k_t}$ as a Törnqvist index, following OECD (2009), starting from $\dot{\overline{k_t}}$ with the base year 1969 and an initial value of 100. The equations characterizing gross capital stock growth as well as capital utilization costs for capital good j are given as

$$\dot{v_t}^j = \dot{v_t}^{j+} - \dot{v_t}^{j-} \tag{7}$$

$$\overline{c_t}^j = \max(0, \overline{r_t} + \overline{\delta_t}^j - \mathbb{E}(\overline{d_t}^j)), \tag{8}$$

where (omitting the time index t)

- k^j denotes use of capital,
- v^j denotes gross fixed assets of capital good j,
- v^{+j} (v^{-j}) denotes additions (disposals) to gross fixed assets of capital good j,
- c^j denotes capital costs of capital good j,
- c^{j-} denotes total capital costs less than capital costs of capital good j,
- r is the required return to capital,
- δ^j is the depreciation rate of capital good j, and
- $\mathbb{E}(d^j)$ is the expected return to capital good j.

The required return to capital $\boldsymbol{r}$ derives from the zero-profit condition

$$(1-\alpha)y_t = r_t v_t^j, \tag{9}$$

i.e., from an aggregate perspective, return to capital cannot be smaller or larger than the capital share of output over gross fixed assets. The depreciation rate can be computed as volume of depreciation for capital good j in t over volume of net fixed assets of capital good j in t. Finally, as we assume rational agents with full information, we approximate expected returns (approximated by the capital good specific investment deflator) by the current (estimated) trend growth rate.

To obtain real disposals and depreciation volumes, we adopt the approach of the Federal Statistical Office and implement the perpetual inventory method (OECD 2009, Schmalwasser and Schidlowski 2006). That is, the distribution of the real disposals (i.e. the mortality function of investments) of investment year i is derived from the density function of the gamma distribution as

$$\boldsymbol{p}(\tilde{n}, n, a, b) = \frac{a^b}{\Gamma(b)} \tilde{n}^{-b} n^{b-1} exp\left(\frac{-an}{\tilde{n}}\right). \tag{10}$$

This density has two strictly positive hyperparameters, namely the rate parameter a and shape parameter b, that control its skewness. For most capital goods, the Federal Statistical Office office assumes $a = b = 9$ (Schmalwasser and Schidlowski 2006). Further assumptions on the average service life $\tilde{n}$ and the service life n that determine the distribution of real disposals. For a given reporting year t, the total real disposal volume obtains as cumulated sum of the real disposals of the previous i investment years with a service life of n = t – i years. Table 1 summarizes our assumptions on the service years and distribution parameters that are calibrated to match the data and the available

information on the service life by the Federal Statistical Office.

We use long-run investment series (that incorporate information on investment in the German Democratic Republic as well as in West Germany prior to 1990) provided by the Federal Statistical Office for construction and equipment in order to achieve a close match to the official disposal and depreciation data after 1990.

	Equipment	Residential Buildings	Non-Residential Buildings	Other Capital
Average length of service life (years)	15	83	49	5
a	9	7	8	9
b	9	7	8	9

Table 1 Parameters of disposal distribution for each capital good. The service life of equipment and residential buildings are time-varying, based on confidential information by the Federal Statistical Office. We report the means.

It is then straightforward to derive the real depreciation volumes as straight line depreciation where the depreciation value in the investment and disposal year is only half the full-year value,

$$v(n) = \begin{cases} \dfrac{1}{2n} & \text{t} = \text{i or t} = \text{i} + \text{n} \\ \dfrac{1}{n} & \text{else.} \end{cases} \tag{11}$$

Thus, depreciation volumes for year n for a given investment year i obtain as $1 - \sum_{n=0}^{i} \boldsymbol{p}(\tilde{n}, n, a, b)$ multiplied with the initial investment in year i and depreciation volumes in year t obtain as cumulated depreciation volumes for investment years i (Schmalwasser and Schidlowski 2006).

3 Estimation and Projection

Estimating Eqs. (1) – (6) directly is a highly challenging and resource-intensive task. Therefore, we employ an approach that is inspired by methods used by institutions like the European Commission and the US Congressional Budget Office: Instead of estimating the entire model in one go, we break it down into its individual components, and Eqs. (1) – (6) serve as the rules of aggregation. However, various challenges arise.

A growing field of research on long-run forecasting highlights the critical importance of including measures of uncertainty in long-term economic forecasts. Müller and Watson (2016) adopt a comprehensive dual methodology, integrating both Bayesian and frequentist approaches, to examine and forecast long-run trends in crucial macroeconomic variables, such as GDP growth rates and population trends. This method effectively addresses stochastic growth patterns and slow mean reversion, while also pointing out the significant uncertainties in projections extending from 10 to 75 years. Similarly, Müller et al. (2022) use a Bayesian factor model to investigate the prolonged growth of GDP per capita across 113 nations over 118 years, offering predictive distributions for their future economic performance over the next century. Again, this analysis underscores the profound

uncertainty in predicting economic growth over extended periods, despite the analysis of detailed historical data.

Our work introduces a further challenge for long-run forecasting: unlike previous studies, we aim to predict an unobserved quantity – potential output – over an extensive time horizon. This task is complicated by the fact that observed data on inputs and outputs are influenced by cyclical variations due to business cycle effects. Consequently, in a first step, we must decompose observed output y_t into its potential component $\overline{y_t}$ and its cyclical counterpart $\tilde{y}_t$. Similar needs arise for capital and labor inputs. Many production function approaches, such as the approach by the European Commission often employ the Hodrick and Prescott (1997) filter to differentiate between transient and permanent signals (Havik et al. 2014, Shackleton 2018, Chalaux and Guillemette 2019, Breuer and Elstner 2020). However, this approach has serious shortcomings. For instance, due to their susceptibility to significant revisions (Orphanides and van Norden 2002, Hamilton 2018, Quast and Wolters 2022, Berger and Ochsner 2022), these filters methods yield unreliable signals. Moreover, they may oversimplify the uncertainty estimation, e.g. due to omitting parameter uncertainty. Such limitations present considerable challenges for policymakers focused on long-term strategic decisions.

We tackle these issues by specifying an alternative filtering algorithm to separate cyclical fluctuations from long-term trends.[1] Bayesian estimation in the spirit of Chan and Jeliazkov (2009) and Mertens (2023) enables the reliable estimation and prediction of uncertainty – including uncertainties about parameters and latent states –, as emphasized by Müller and Watson (2016) and Müller et al. (2022). For a time series x_t, our signal extraction problem is characterized by a system similar to that of Chan et al. (2013), i.e.

$$x_t = x_t^\tau + x_t^c \tag{12}$$

$$x_t^\tau = x_{t-1}^\tau + x_t^g + \eta_t^\tau \qquad \eta_t^\tau \sim \mathcal{TN}\left(0, \sigma_\tau^2\right)_{\left[\underline{x_t^\tau} - x_{t-1}^\tau, \overline{x_t^\tau} - x_{t-1}^\tau\right)} \tag{13}$$

$$x_t^g = x_{t-1}^g + \eta_t^g \qquad \eta_t^g \sim \mathcal{N}\left(0, \sigma_g^2\right) \tag{14}$$

$$x_t^c = \phi_t x_{t-1}^c + \eta_t^c \qquad \eta_t^c \sim \mathcal{N}\left(0, \exp\left(\psi_t\right)\right) \tag{15}$$

$$\phi_t = \phi_{t-1} + \eta_t^\phi \qquad \eta_t^\phi \sim \mathcal{TN}\left(0, \sigma^\phi\right)_{[0-\phi_{t-1}, 1-\phi_{t-1})} \tag{16}$$

$$\psi_t = \psi_{t-1} + \eta_t^\psi \qquad \eta_t^\psi \sim \mathcal{N}\left(0, \sigma_\psi^2\right) \tag{17}$$

where $\mathcal{N}$ denotes the normal distribution, $\mathcal{TN}$ denotes the truncated normal distribution, and the innovation distribution subscript in Eq. 13 indicates bounded support.

The innovations are mutually orthogonal across Eqs. 12 – 17 in all $t = 1 \ldots T$ and $\underline{x_t^\tau}$ and $\overline{x_t^\tau}$ are known constants. For an in-depth understanding of the precision sampler employed to differentiate between trends and cycles and to project the trends into the distant future, please refer to Appendix G. Our sample begins in 1970 and incorporates the short-run business cycle forecasts for investment, deflators, unemployment and average working hours for the current and the next year as data.[2] Table 2 summarizes the information on data. Note that the system of Eqs 12–17 gives rise to a straightforward

[1] A few series, treated as random walks, are exceptions. See Appendix H

[2] For prior specifications and detailed estimation results, see the Technical Appendix.

way to project trends and cycles into the future by drawing from the innovation distributions and iterating on the state equations. Regarding our projection methodology, we forecast all components except for the population, which we source from the population forecast by the Federal Statistical Office. Thus, population dynamics are entirely exogenous to our model. The scenario of the Federal Statistical Office underlying our baseline specification assumes an average birth rate of 1.55 children per woman, a gradual but moderate increase in life expectancy until 2070, and an average net migration of 250,000 people starting in 2033.

Name	Description	Time period	Unit	Source
Average years of schooling	Average years of schooling	1960 – 2015	Number of years	de la Fuente and Doménech (2006)
Commuter balance	Difference of incoming and outgoing commuters	1970 – 2022	Number of persons	Federal Statistical Office
Investment deflator	Real investment deflators for all capital goods	1970 – 2022	Chain index	Federal Statistical Office
Historical hours	Total hours worked	1970 – 1990	Number of hours	Federal Statistical Office
Hours	Hours worked by part-time, full-time and self-employed workers	1991 – 2022	Number of hours	Institute for Employment Research
Real investment	Real investment volumes into capital stock for all capital goods	1970 – 2022	Billion euros, chained volumes, base year = 2015	Federal Statistical Office
Real gross capital stock	Real gross capital stocks for all capital goods	1970 – 2022	Billion euros, chained volumes, base year = 2015	Federal Statistical Office
Real net capital stock	Real net capital stocks for all capital goods	1970 – 2022	Billion euros, chained volumes, base year = 2015	Federal Statistical Office
Real depreciation	Real depreciation volumes for all capital goods	1970 – 2022	Billion euros, chained volumes, base year = 2015	Federal Statistical Office
Real disposals	Real disposal volumes for all capital goods	1991 – 2022	Billion euros, chained volumes, base year = 2015	Federal Statistical Office
Real gross domestic product	Real gross domestic product	1970 – 2022	Billion euros, chained volumes, base year = 2015	Federal Statistical Office
Part-time employment	Number of part-time employed workers	1991 – 2022	Percent	Institute for Employment Research
Population	Population data as of January 1 of each year by age and gender	1960 – 2022	Number of persons	Eurostat
Population projection	Population projection as of December 31 of each year by age, gender and various projection assumptions.	2022 – 2070	Number of persons	Federal Statistical Office
Self-employment	Number of self-employed workers	1991 – 2022	Percent	Institute for Employment Research
Working population	Working population by age group and gender	1970 – 2022	Number of persons	OECD

Table 2 Information on data. All data are sampled at yearly frequency, except for the data from de la Fuente and Doménech (2006), which are sampled in five-year intervals. All capital goods refer to equipment, residential and non-residential as well as other capital, respectively. Data before 1990 refer to West Germany. We account for German reunification by re-chaining the West Germany data to the 1991 data of the Federal Republic of Germany.

The filter specified in Eqs. 12–17 builds upon a broad consensus in the broadly empirical literature about the properties of macroeconomic series, especially regarding the merits of stochastic trend models, as in Eq. 13 for key economic measures like inflation and unem-

ployment (see, e.g. Smets and Wouters 2007, Chan et al. 2013, 2016) or output (Morley et al. 2003, Grant and Chan 2017a,b, Chan et al. 2019) as well as total factor productivity (Chan and Wemy 2023). Moreover, Chan et al. (2013, 2016) suggest that bounded trend models are effective for modeling and forecasting unemployment and inflation. In our application, bounded trend estimation is needed, e.g. in the case of filtering rates, by definition, that lie between zero and one-hundred, which would be hard to achieve by alternative transformations (for instance, the log-transformation would only avoid negative values, but would enable estimation of aggregates that are bounded from above). The precise nature of trend growth for macroeconomic aggregates (Eq. 14) remains debated, particularly regarding the occurrence and timing of breaks (for instance, in the case of output, various specifications with and without breaks, are discussed e.g. in Morley et al. 2003, Grant and Chan 2017a,b, Berger and Kempa 2019). Considering various economic aggregates, including labor and capital inputs, to predict potential output, we adopt a more agnostic, stochastic approach to trend growth, as displayed in Eq. 14.

We use the trend growth specification in Eq. 14 for all capital- and TFP-related series. Note that $\mathbb{E}(x_{t+1}) = x_t$. However, since some labor-market indicators display negative trend growth, this characteristic will inevitably pose challenges when forecasting these indicators. When trend growth is consistently negative, an infinite sum of such values approaches its lower bound (or negative infinity if there is no specified lower bound) in the limit. In many economic contexts, this assumption is not reasonable or practical. For instance, several indicators related to working hours exhibit negative trend growth. Using Eq. 14 in such cases would imply that average working hours will eventually reach its lower trend bound zero. However, zero average working hours would imply that potential output is also zero, which is not a well-grounded belief.

To ensure that our model is well-behaved in the limit and does not lead to unrealistic outcomes, we aim to exclude these problematic cases. Therefore, we deviate from the baseline filter for labor series and use the mean-reverting trend growth specification

$$x_t^g = \mu + \phi^g x_{t-1}^g + \eta_t^g \qquad \eta_t^g \sim \mathcal{N}\left(0, \sigma_g^2\right), \tag{18}$$

with ϕ^g on the complex unit circle, such that $\mathbb{E}(x_{t+1}) = \dfrac{\mu}{1-\phi^g}$.[3] Similarly, when trend growth as given by Eq. 14 is positive, it implies summing over positive values in the limit. From an economic theory perspective, this behavior is desirable, especially for TFP. However, to ensure that the accumulation of capital is realistic and accounts for its finite service life, we employ a vintage structure, where capital goods exit the capital stocks based on their disposal and depreciation distributions. These distributions are derived from a Gamma density that is governed by the average service life specific to capital goods.[4]

A further noteworthy feature of our specification is its incorporation of a stochastic volatility component within the cycle (Eq. 15), as discussed by Kim and Nelson (1999). This

[3] In a Bayesian context, the additional estimation of μ and ϕ^g is simple and does not impose too much computational burden; μ is a linear regression parameter and for estimating ϕ^g, we refer to Chib and Greenberg (1994).

[4] For more information, please refer to Appendix C.

addition of stochastic volatility enhances the decomposition's resilience against significant economic shocks (Berger et al. 2016, Chan et al. 2016, Berger and Kempa 2019), such as those witnessed during crises like the COVID-19 pandemic (2020-21) or the recent energy crisis in 2022. The time-varying parameter ϕ_t plays a critical role in determining the persistence of the cyclical process, as in Chan et al. (2016).[5]

All of our priors are derived from a straightforward, conjugate normal-gamma framework. In our trend-cycle decomposition, we often calibrate the initial conditions of the trend and set relatively informative priors on the initial conditions of trend growth and their innovation variances. Overall, our approach to these priors strikes a balance between using prior knowledge where it is available and allowing the model the freedom to adapt and learn from the data. This helps us achieve convergence in a reasonable amount of time. Additionally, using priors that focus on small values for innovation variances aligns with economic theory, which suggests that potential and potential growth in macroeconomic aggregates are slow-moving signals compared to business cycle fluctuations. Regarding the cyclical components, we typically set loose priors on the stochastic volatility components and, if applicable, on autoregressive coefficients. For the second model class, random walk models, our priors are generally quite lenient.

After estimating the individual components, we employ Eqs. 1 – 6 as aggregation rules for the estimated trend components. This approach, commonly used in the literature and at policy institutitions and (international) organizations such as the OECD (Chalaux and Guillemette 2019), the European Commission (Havik et al. 2014) and the German Council of Economic Experts (Breuer and Elstner 2020). However, unlike the aforementioned institutions that rely on the Hodrick and Prescott (1997)-filtered means of the trends, we apply this procedure to the entire distribution samples. This comprehensive procedure enables us to derive estimates of the distributions for $\overline{l}, \overline{h}, \overline{k}$, and $\overline{a}$, ultimately leading to our estimation of $\overline{y}$.[6] Subsequently, we extract robust statistics, such as the median along the time dimension from these distribution samples, facilitating point-inference. Whereas the median of the predictive distribution serves well as 'the' expectation of German economic growth, we can derive optimistic (pessimistic) expectations from quantiles above (below) the median quantile.[7]

[5]In addition, specifying the persistence parameter to be time-varying achieves that revisions are less likely and less severe, as each parameter for a given time t is only determined by its own past and the current data, such that new extreme observations do not lead to large parameter revisions for data in the distant past.

[6]In total, our process entails estimating 29 disaggregated variables, including factors like equipment investment and labor participation segmented by age groups. For more details, please refer to the Technical Appendix. Given that we obtain 360,000 draws from over 300 (partly multivariate) conditional posteriors, discard the initial 10,000 as burn-in, and only retain every seventh draw to enhance convergence, this process demands a considerable amount of time and necessitates hardware capable of running multiple models concurrently.

[7]Note that while the individual components, obey (truncated) (log-)normal distributions (see Technical Appendix), the nonlinear transforms $\overline{l}, \overline{h}, \overline{k}, \overline{a}$, and $\overline{y}$ of these normal samples do not. Therefore, their distribution samples can (but not necessarily need to) have non-zero skewness, which is a very useful feature when it comes to judging economic risks.

4 Demographic Dynamics and German Potential Output Growth 1970 – 2022

In this section, we discuss estimation results with a particular focus on how demographic dynamics have shaped the labor input and thereby potential output in the estimation period that spans 1970 to 2022. Recall that population size affects labor volume growth by altering components like the labor force and the aggregated labor participation rate. The latter is a weighted average of age-group specific labor participation rates (see Eq. 3).

Potential output and gross domestic product

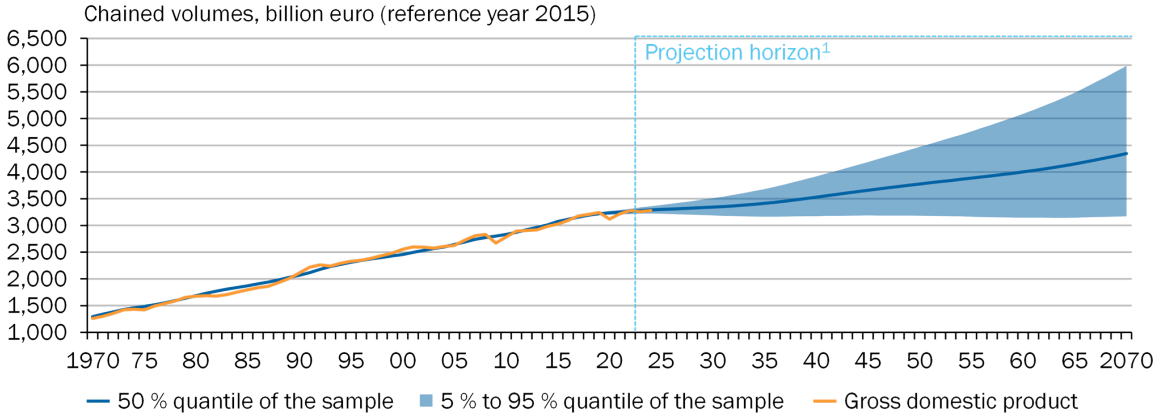

1 – Values for 2023 and 2024 are based on the German Council of Economic Experts' short-term forecast. From 2025 projection.

Sources: Federal Statistical Office, IAB, OECD, own calculations
© Sachverständigenrat | 23-283-01

Figure 2

Figure 2 displays estimated German potential output alongside gross domestic product (GDP) and Figure 3 shows the contributions of capital, labor, and TFP to potential output growth. First of all, note that the real growth rate of Germany's potential output has declined significantly over the years, from approximately 3.3% at the onset of the estimation period in 1970 to around 0.5% in 2022. It averaged 1.5% per annum in the decade between 2010 and 2019. However, potential output growth experienced a temporary peak in 2022, driven by a net population influx of approximately 1.5 million people during that year. Various factors contributed to the slowdown in the growth rates of potential output since 1970.

The overall decline aligns with the literature that finds a tendency for economies to converge towards their long-run (i.e. steady-state) growth rates in the absence of shocks. The convergence in economic growth is attributed to two primary factors, as identified in the literature. Firstly, neoclassical and newer theoretical models (Ramsey 1928, Solow 1956, Barro and Sala-i Martin 1997, Acemoglu 2006), propose that capital growth per capita converges to a steady state, a phenomenon that is also empirically validated (Barro and Sala-i Martin 1991, Barro 2015). Secondly, recent research indicates a constant reduction

in TFP growth in developed economies over time. The difficulty in discovering new ideas for research and development leads to a decrease in innovations and, consequently, TFP (Gordon 2012, Bloom et al. 2020). Consistent with this literature, substantial decreases in the growth rate of TFP have played a significant role in the decline of potential output growth, also for Germany.[8] The trajectory of TFP growth in Germany has been consistently downward since at least the late 1990s. According to our model, TFP's trend growth slowed significantly from around 1.0% in 1999 to 0.3% in 2011, and it has remained at this lower level since. This trend aligns with a broader productivity slowdown observed in numerous advanced economies, influenced by a combination of factors (Bloom et al. 2020, Goldin et al. forthcoming). In addition, studies highlight that innovations elevate growth more strongly when production factors are efficiently allocated (Restuccia and Rogerson 2008, 2017), but evidence suggests a decline in allocation efficiency over time (Gopinath et al. 2017).

Growth contributions of components to potential output

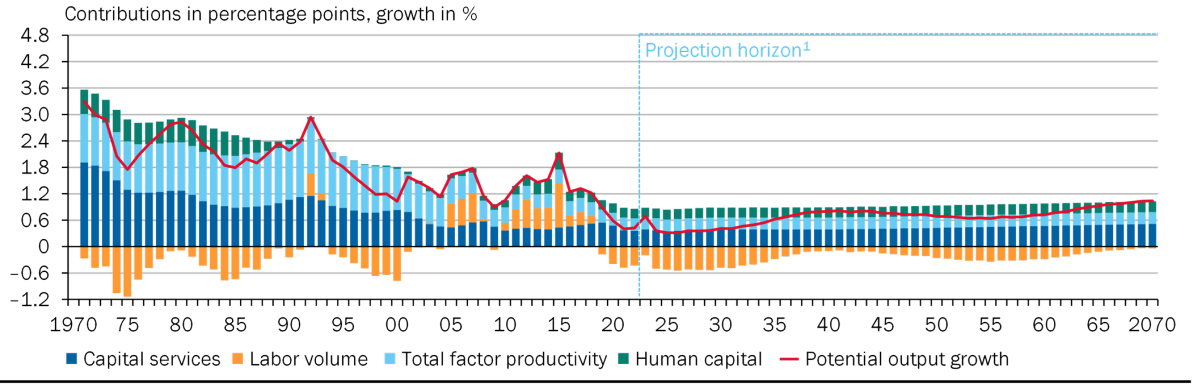

1 – Values for 2023 and 2024 are based on the short-term forecast by the GCEE. From 2025 projection.

Sources: Federal Statistical Office, IAB, OECD, own calculations
© Sachverständigenrat | 23-170-03

Figure 3

Throughout most of the sample period, the labor volume's contribution to potential output growth remained negative (see Figure 3, orange bars). Notably, potential labor, measured in hours, experienced contraction from 1970 to 1999, resulting in an average reduction of potential growth by about 0.5 percentage points per year. However, reductions of potential output growth due to negative labor volume growth were much more pronounced during the 1970s and 1980s. To investigate the main drivers of this decline, we decompose labor volume growth $\dot{\bar{l}}$ in the spirit of Eq. 4 into contributions from working-age population dynamics $\dot{\bar{b}}$, labor participation $\dot{\bar{w}}$, structural unemployment $\dot{\bar{u}}$ and average hours worked $\dot{\bar{h}}$.

[8] Our TFP growth estimates, accounting explicitly for the accumulation of intangible assets and human capital formation, are generally lower than those in other studies (e.g. Havik et al. 2014).

Growth contributions of components to labor volume growth

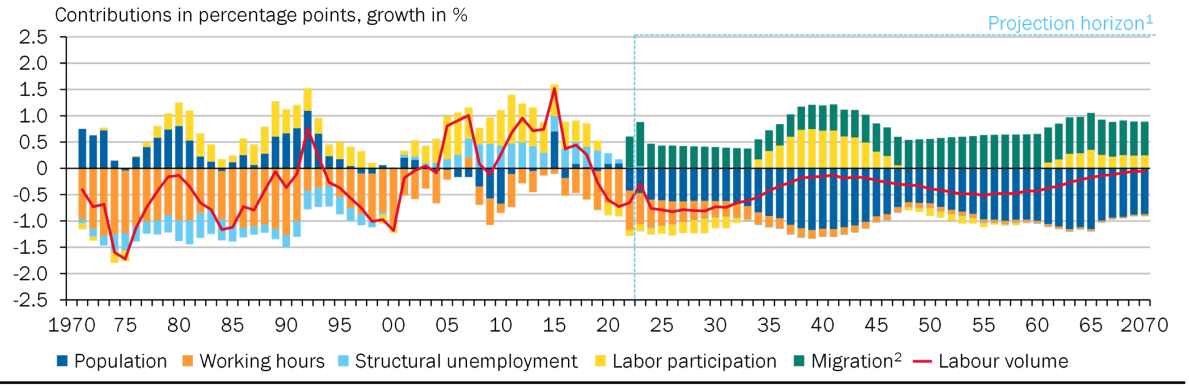

1 – Values for 2023 and 2024 are based on the short-term forecast by the GCEE. From 2025 projection, results of the reference scenario. 2 – From 2022 explicitly modeled; 1970 – 2021 included in population.

Sources: Federal Statistical Office, own calculations

Figure 4

Figure 4 reveals considerable fluctuations in the underlying labor components. Interestingly, the primary factor behind this decline was the consistent decrease in average working hours, contributing an average of -0.9 percentage points to the labor volume annually. Despite this, the overall impact on the aggregated labor volume during the observation period was tempered by an expanding working-age population (+0.4 percentage points per annum) and an increasing labor participation rate (+0.2 percentage points per annum). A consequential effect of the contracting (equilibrium) labor volume is the gradually increasing marginal product of labor, as depicted in Figure 5 (left panel). Consistent with the reduced availability of labor, we observe a decrease in cross-partial derivatives (right panel) of the production function in Eq. 1, signaling a lower productivity of inputs. While the labor volume was depressing economic growth between 1970 and 2000, it became a growth driver from the onset of the millennium until 2019. This can be attributed, in part, to a significant reduction in the natural rate of unemployment, dropping from 8.4 percent in 1999 to 2.4 percent in 2022, following the labor market reforms of the 2000s (Hochmuth et al. 2021). Concurrently, the labor force participation rate increased from around 65% to approximately 70%.

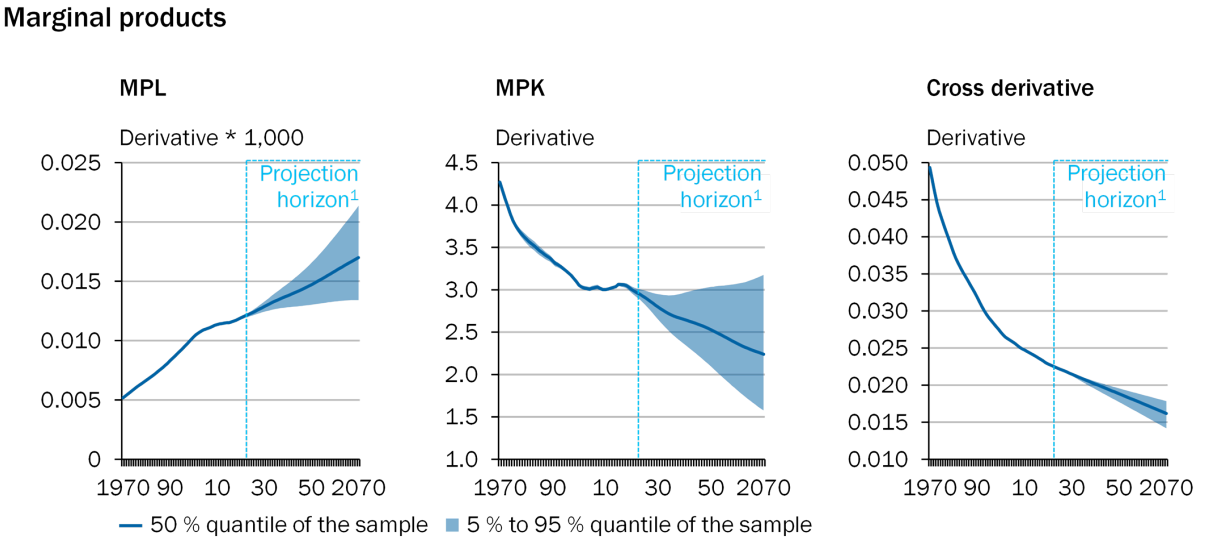

1 – Values for 2023 and 2024 are based on the short-term forecast by the GCEE. From 2025 projection, results of the reference scenario.

Sources: Federal Statistical Office, IAB, OECD, own calculations
© Sachverständigenrat | 23-507-01

Figure 5

However, these favorable conditions gradually diminished as the labor market approached saturation in the 2010s. Since 2019, the contribution of the labor volume to growth has once again turned negative. The decline in average working hours has been accelerating since the mid-2010s, and the retirement of the baby boomers has begun to dampen labor volume growth. Consequently, the labor volume contracted by 0.7% in 2022. As the peak impact of increased migration flows due to Russia's war of aggression against Ukraine on the working-age population is anticipated in 2023, the decline in the labor volume is expected to decelerate in 2023 before resuming at a rate of -0.8% per annum for the remainder of the decade.

Figure 6 illustrates the breakdown of growth in capital services $\dot{\bar{k}}$ (for more details, see Appendix C). The accumulation of tangible fixed assets and their utilization in the production process has significantly fueled the expansion of potential output since the 1970s. Capital service growth, with few exceptions, has been the primary contributor to potential growth, averaging a growth contribution of 0.8 percentage points per year since that time. For instance, in 2022, the contribution of capital services to potential growth was 0.4 percentage points. While the growth contributions of capital services have consistently been positive in the past, they are showing a declining trend over many years, except for other capital, primarily intellectual property. Notably, the growth contributions of non-residential buildings, such as factories or roads, have approached zero since the turn of the millennium. Despite the marginal product of capital experiencing a decline until the early 2000s, it has more or less stagnated over the last two decades (see Figure 5, middle panel).

Contributions of components to capital services growth[1]

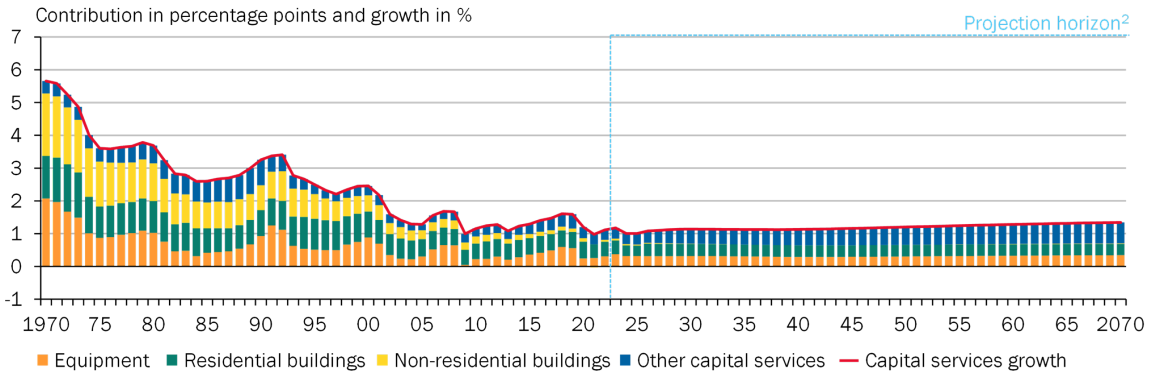

1 – 50 % quantile of the sample is shown. 2 – Values for 2023 and 2024 are based on the short-term forecast by the GCEE. From 2025 projection.

Sources: Federal Statistical Office, own calculations

Figure 6

5 Demographic Aging and the Future of Economic Growth in Germany

Our projection reveals an average annual growth rate of 0.7% for potential output from 2023 to 2070 (see Figure 3). However, the projected average growth rates for the 2020s and 2030s are much lower, with 0.4 % and 0.5%, respectively. In line with Müller and Watson (2016) and Müller et al. (2022), we find substantial uncertainty around our estimates (see Figure 2). More precisely, by 2070, potential output would grow cumulatively by between -0.2 % (5 % quantile of the simulated trajectories) and 2.4 % (95 % quantile of the simulated trajectories) compared to 2022. Thus, it is therefore rather unlikely that potential output will fall below the current level in the long term. However, it seems just as unlikely that there will be a similarly strong increase as between the years 1970 and 2022.[9] Nevertheless, the findings indicate a significant slowdown in potential output growth for the next 50 years compared to the previous half-century. With growth projected to be less than linear (see Figure 2) over this extensive period, it signifies a decline in economic prospects spanning a generation.

Our projections provide important insights into the labor market outcome of the demographic transition (see Figure 4). The diminishing working-age population will impact potential growth in the decades to come. Moreover, despite a substantial decrease in the structural unemployment rate from 2005 to 2018, it is not expected to decrease any further. Moreover, a continuous reduction in full-time hours is anticipated to result in negative growth contributions from working hours. The baseline projection also suggests that part-time and self-employment rates will stabilize near current levels, at around 40% and 8%, respectively, until 2030, both with adverse effects on average working hours. Finally, the labor participation rate is expected to rise from 69% in 2022 to 75% in 2070.

[9] More details on distributional estimates of potential output, its growth rate and the output gap can be found in Appendix F.

In addition, the model anticipates a 0.4 percentage point yearly contribution of capital investment to potential output growth (see Figure 3), with other capital expected to contribute almost 28% to capital services by the end of the projection period (see Figure 14, left panel). This would indicate a major shift in the capital service composition. Conversely, the capital service share of non-residential buildings is projected to decline from 35% in 1970 to 13% in 2070. The projected increase in labor scarcity is accompanied by steady increases (decreases) in its marginal product (the cross derivative), as shown in Figure 5. The projected increase (decrease) of the marginal products imply, ceteris paribus, higher (lower) real future labor (capital) compensations, at least in the very long-run and in the absence of aggregate market concentration.

5.1 The Transmission of Demographic Shocks

By analyzing the breakdown of labor growth in Figure 4, we can understand the extent to which the two external factors in the model, i.e. domestic population dynamics and migration, are *causing* potential output to decrease via a reduction of the labor force. To see the causal nature of population effects on labor participation and the labor force in the model, recall that, abstracting from migration, population is determined by birth and death rates. As the working age in our analysis starts at an age of 15 years, the birth rate of $t-15$ and earlier in the past should be uncorrelated with innovations to potential output in t. Assuming further that the death rate in t does not fluctuate too much, domestic population and migration dynamics likely allow for a structural, i.e. causal interpretation. However, variation in the remainder of the labor market aggregates does not lend itself to a straightforward causal interpretation.

It is possible that demographic changes can transmit via labor market aggregates, such as the number of working hours, that are not mechanically linked to population dynamics in our model. These effects would escape the causal structure. To investigate how demographic shocks might translate into labor aggregates, we construct an auxiliary dynamic structural model. In this model, we represent our collection of time series as z_t, with z_t being a vector with dimensions $K \times 1$. We consider both the reduced form and its structural counterpart in the system

$$\begin{aligned} z_t &= \nu_t + A_1 z_{t-1} + \ldots + A_p z_{t-p} + u_t && (19) \\ &= \nu_t + A_1 z_{t-1} + \ldots + A_p z_{t-p} + B\varepsilon_t, \ t = 1, \ldots, T, && (20) \end{aligned}$$

respectively, where $A_j, j = 1, 2, \ldots, p$, are $K \times K$ coefficient matrices and ν_t is a $K \times 1$ dimensional vector of intercepts. Reduced form residuals u_t in (19) are serially uncorrelated with mean zero and non-diagonal covariance matrix Σ_u. By assumption, structural shocks ε_t in (20) have identity covariance, $\varepsilon_t \sim (0, I_K)$, such that $\Sigma_u = BB'$. Finally, z_t has a Wold moving average (MA) representation, and hence, causality obtains.

This system is straightforward to estimate by means of least-squares algorithms. We set $p = 1$. The median response as well as 68% and 90% confidence bands are derived from a residual-based fixed-design moving block bootstrap in the spirit of Brueggemann et al. (2016), which has the advantage of consistently handling non-Gaussian, possibly heteroskedastic, shocks over 30 horizons. Using population dynamics to identify the

effects of the German demographic transition on working hours, is unlikely to yield the desired outcome. Instead, to approximate the effect of aging, we require a mapping from population composition by age-groups to the real line. To this end, we use the old-age-dependency ratio (i.e. the ratio of persons aged 65 years or older to the remaining working-age population).

Due to the few observations in the yearly-frequency time dimension, we construct two systems. The first model, SVAR 1, focuses on labor market aggregates, i.e. old-age-dependency ratio, participation, and unemployment data (represented in natural logarithms and scaled by 100). The purpose of this model is to investigate whether the transmission pattern from aging shocks to labor participation (see previous Section) correctly shows up in aggregate models – which may increase our confidence in identification – and to learn about a possible transmission into unemployment. This system spans from 1970 to 2014, thus excluding the notable migration inflows of 2015, and arranges these aggregates below the German old-age-dependency ratio. Identification of the system is done recursively. In addition, SVAR 2 focuses on the disaggregated average working hours, encompassing part-time rates and both full-time and part-time hours, sampled from 1991 to 2020. Similar to SVAR 1, we order these disaggregates below the German old-age-dependency ratio and identify the system recursively.

In both models, an aging shock refers to an increase in the old-age dependency ratio by 1% immediately following impact. Prior to estimation, the data in both models undergoes orthogonalization to a quadratic trend by means of linear projection. Figure 7 depicts the median as well as 68% and 90% probability mass of the bootstrapped identified impulse responses. The first column of Figure 7 shows the results from SVAR 1. The dynamic response patterns of the working-age population and labor participation are indeed as expected (first and second rows, first column). While the working-age population decreases about 0.1% after 5 horizons, labor participation decreases on impact by the same amount. In particular, since our labor force participation rate includes the age bracket 15–74, and workers aged 65 or older have extremely low participation rates, the aggregate labor participation rate decreases. Interestingly, the unemployment rate (third row, first column) seems to decrease in the long run (after 12 horizons), possibly pointing to an increased scarcity of workers in aging societies. Overall, the findings from SVAR 1 lends support to the identification scheme, as they are well aligned with prior expectations and the baseline projection model.

Dynamic responses of labor aggregates to aging[1]

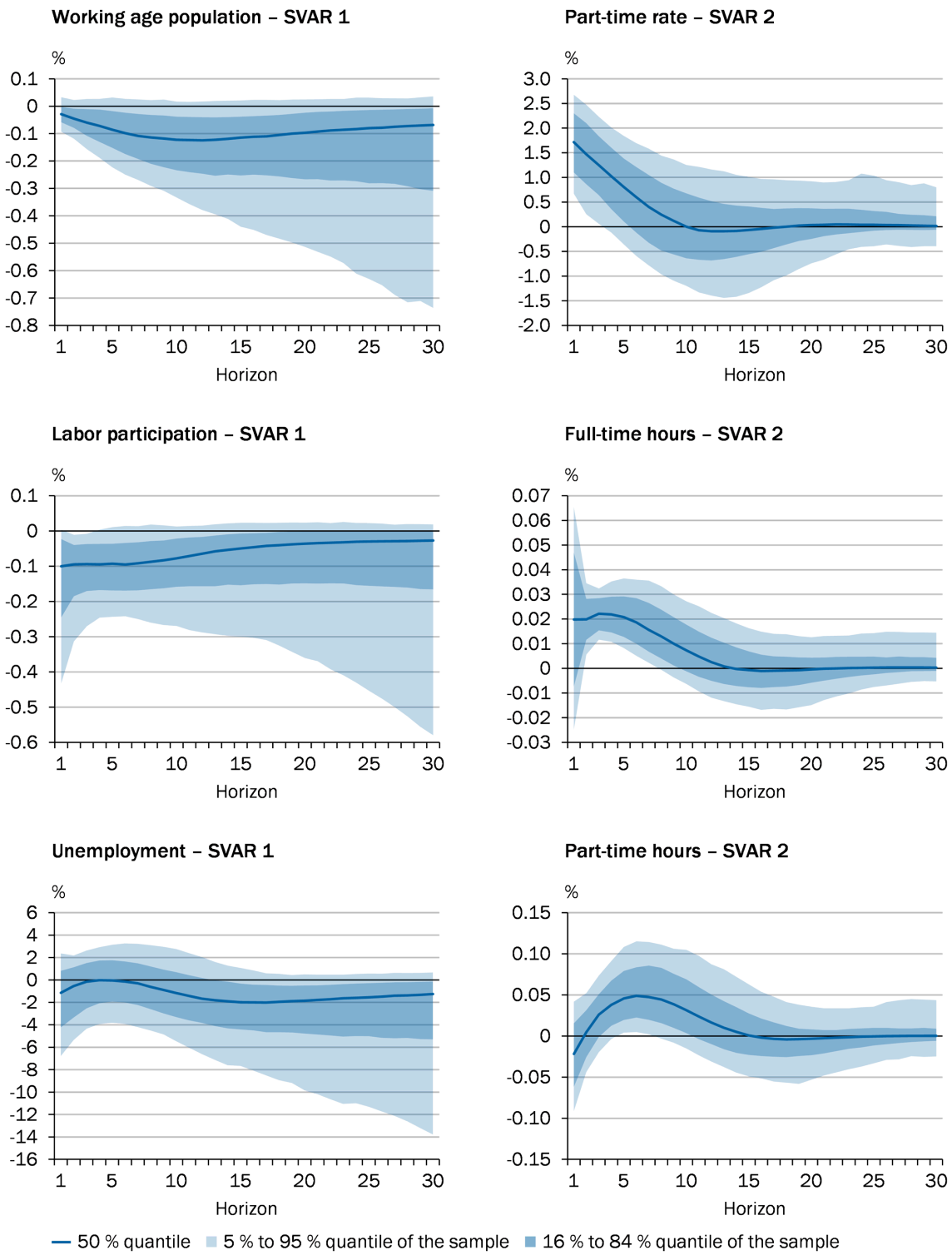

1 – Sample in SVAR 1 from 1970 to 2014. Sample in SVAR 2 from 1990 to 2020.

Sources: Federal Statistical Office, own calculations

Figure 7

The second column of Figure 7 depicts the results from SVAR 2.[10] Interestingly, the part-time rate and the hours (full-time and part-time) increase for about 15 horizons each. Whereas the part-time rate (first row, second column) increases on impact by almost 2%, the effects on hours are a lot less pronounced. Importantly, the effect pattern implies an ambiguous effect on average working hours, as full-time working hours and part-time working hours increase average working hours, ceteris paribus. The effect patterns align well with micro-data at our disposal (see next Section). In particular, working hours data reveals that the age-group 65 and older has the highest full-time and part-time working hours of all age groups. In a similar vein, this is also the group with the highest, part-time rate. Thus, in all three cases, the model points towards composition effects where older workers with particular labor market characteristics gain more weight in the aggregates.

5.2 A Micro-Data Perspective on labor Shortage

Given the ambiguous transmission of aging shocks into average working hours, as indicated by our impulse response exercise, it becomes crucial to differentiate between overall reductions in working hours (i.e., a collective decrease in working hours among all workers) and composition changes (i.e., a higher proportion of workers either reducing their hours or opting for part-time arrangements). This distinction is vital for assessing the prospective trajectory of hours worked.

For this purpose, we utilize disaggregated hours data sourced from the Institute for Employment Research. This data spans from 1991 to 2022 and encompasses working hours by full-time, part-time, and self-employed workers, categorized by gender and age-cohorts at five-year age brackets. This dataset underscores the significance of both factors in explaining the observed decline in full-time working hours. For instance, among male full-time employees aged 60 to 64, the average annual working hours decreased from 1670 hours in 1991 to 1535 hours in 2022, a decrease of 8%. Similar trends are evident among female workers, where the 2% decrease is more moderate.

To further explore the underlying reasons for the prolonged decrease in average working hours, we undertake a series of counterfactual analyses. In doing so, we leverage the decomposition of average working hours, recognizing it as a weighted combination of part-time, full-time, and self-employment rates, as outlined in Eq. 4. For clarity, we reproduce the equation here:

$$s_t = s_t^s q_t^s + (1 - q_t^s)(s_t^p q_t^p + (1 - \overline{q_t^p}) s_t^f).$$

It is worth noting that we use the raw data s^* in the following exercises rather than the filtered series $\overline{s^*}$. The data enables us to compute age-cohort-based counterfactuals. For example, we can calculate the hypothetical scenario of average working hours if the relative size of workers' age groups had not changed compared to 1991. While the outcomes of this exercise may not permit a causal interpretation in the 'structural' sense, given that

[10] Upon visual inspection reveals that the identified aging shocks from both SVARs align very well. In addition, they exhibit decent correlations. We obtain correlation coefficients of about 0.4 for linear and rank correlations after the exclusion of one initial outlier, which seems large given the small samples. Overall, we are confident that both models identify the same shocks.

fundamental shocks (such as preference shocks to labor supply) might impact more than one aggregate in Eq. 4, making it challenging to attribute variations within specific aggregates to single fundamental shocks, our results remain highly informative regarding the underlying economic transmission mechanism. Figure 8 compares

- realized average working hours (red line),
- a counterfactual of average working hours where the number of workers per age-group remains at the level of 1991 (orange line),
- a counterfactual of average working hours where the number of working hours per age-group remains at the level of 1991 (light blue line),
- a counterfactual of average working hours where the part-time rate is at the level of 1991 – that is, only 20%, instead of 39% (yellow line), and a counterfactual of average working hours where the self-employment rate is at the level of 1991 – that is, 9.2% instead of 8.6% (dark blue line).

Figure 8 clearly illustrates a significant decline in average working hours from about 1540 hours per worker per year in 1991 to about 1320 hours in 2022 (red line). This translates into a reduction of average weekly working hours by 16% between 1991 and 2022. However, the altered composition of age-brackets, as indicated by the orange line (reflecting an increased number of older workers), appears insufficient to account for this reduction. This implies that demographic shocks apparently did either not transmit via the labor force composition or that they were associated with limited effects on hours in the last three decades.

Counterfactual developments of average hours worked vs. realized development

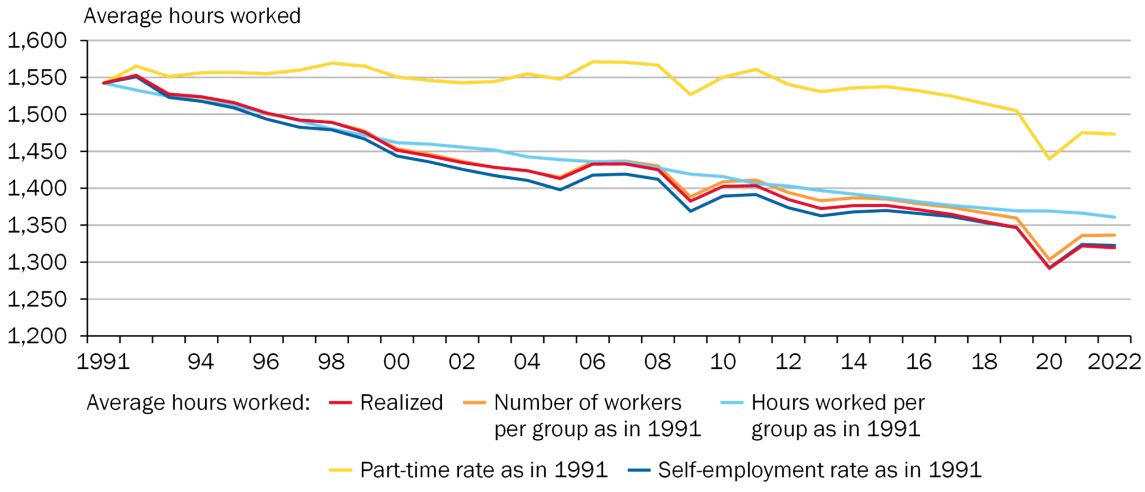

Sources: IAB, own calculations
© Sachverständigenrat | 23-506-01

Figure 8

While the decrease in hours worked within each age group, represented by the light blue line, explains a noteworthy portion of the overall decline, the primary factor behind reduced average working hours seems to be the substantial rise in the part-time rate, soaring from 19% in 1991 to 38% in 2022. In fact, average working hours would be at

1473 in 2022, if the part-time rate still was at 19%, as in 1991. Another 40 average working hours would be added, if average hours worked did not decline across almost all age groups since 1991.

To clarify, although there are observable reductions in full-time working hours, particularly in recent years, the predominant driver of the long-term average working hours decline is a compositional effect—specifically, the growing importance of part-time work arrangements. This shift may be attributed to various factors, including preferences for leisure over work, responsibilities such as childcare and elderly care (largely shouldered by females in the prime working age of 20-59 years in Germany).

To grasp the dynamics of the part-time rate, Figure 9 contrasts several hypothetical scenarios of the part-time rate with the actual observed rate (left panel). Furthermore, the figure displays age-group-specific observed part-time rates (right panel). Evident from both analyses is that, although there is a minor impact from workforce age-composition (as indicated by the orange line in the left panel), substantial increases in the part-time rate across all age groups contribute significantly to the overall rate surge between 1991 and 2022 (as seen in the comparison between the light blue and dark blue lines in the left panel).

Part-time rate decomposition

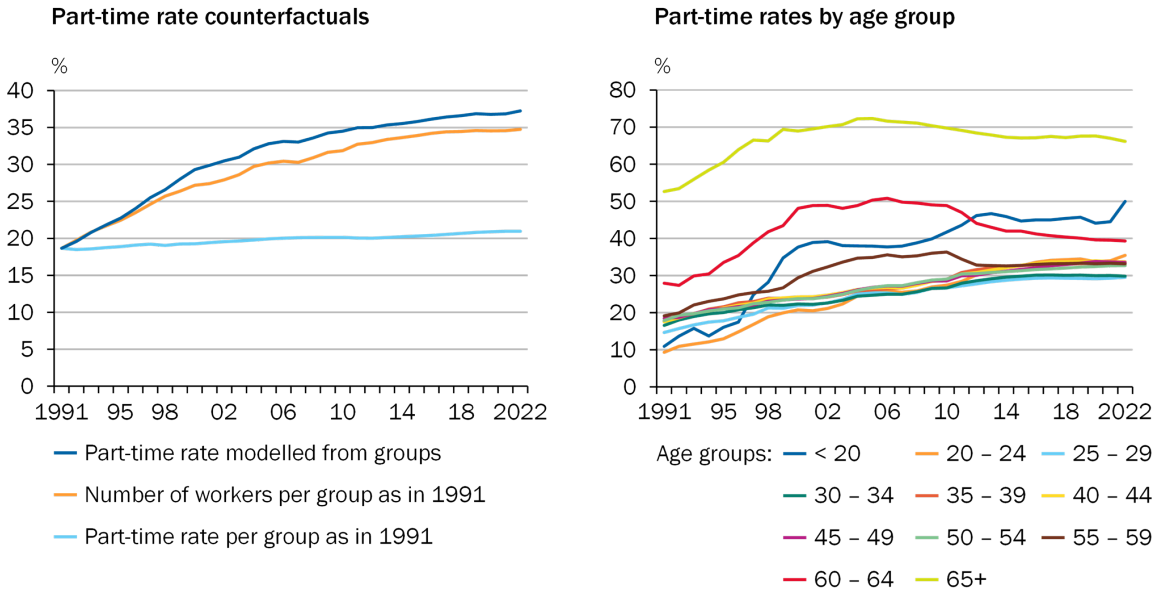

Sources: IAB, own calculations
© Sachverständigenrat | 23-510-01

Figure 9

Nevertheless, notable disparities in both levels and growth rates exist among age groups (right panel). Workers aged 65 or older exhibit the highest part-time rate, which experienced a substantial surge in the 1990s and the beginning of the millennium but has since stabilized around 65%. In contrast, the prime working age groups (20-59 years) demonstrate persistent increases, rising from approximately 10% to around 30% (or slightly

above). Note that the increase in the part-time rate of elderly workers and the implied increase is a prime example of demographic transmission and consistent with the dynamic effects of aging shocks on the aggregate part-time rate, as discussed above.

This pattern aligns with the increased labor force participation of women over the past three decades, predominantly engaging in part-time work. This trend is on the rise. According to our dataset, the part-time rate for women escalated from 33% in 1991 to 54% in 2022. Various factors may contribute to this shift. In particular, women with children may find it unfeasible to offer full-time labor due to care-giving responsibilities and insufficient childcare opportunities (German Council of Economic Experts 2023). Thus, some might be forced to choose part-time employment and consequently elevating the part-time rate.

The overarching conclusion drawn from our examination of average working hours is that elevations (reductions) in the part-time rate present significant risks (chances) to the overall labor volume. Although previous increases cannot be solely attributed to demographic change, the impulse response patterns analyzed in Section 5.1 give rise to the concern that demographic aging will contribute to heightened aggregate part-time rates, ceteris paribus.[11] This is particularly worrisome as the share of older workers, who presently exhibit very high part-time rates, is anticipated to increase dramatically. Consequently, this trend could lead to a depression in average hours, even beyond what is anticipated in the model.

6 Putting the German Economy back on Track

Our modeling approach not only allows to track the propagation of adverse shocks to growth, but it also allows to evaluate policy strategies that may increase growth in the medium to long term. Given our key finding highlighting the unfortunate alignment of low growth in TFP and capital services alongside labor volume reductions resulting from demographic transition, a practical combination of two policy strategies becomes apparent. Firstly, there is a need to enhance investment in capital goods and research to elevate capital services and TFP. Secondly, addressing labor market issues or, at the very least, alleviating the adverse effects of demographic transition is crucial.

[11] Recall that our model does not reflect possible general equilibrium effects. For instance, a larger share of old workers with high part-time rates and retirees may increase the supply of informal child care opportunities, which in turn may reduce part-time rates of prime work-age women. However, note that these effects are unlikely to dominate the overall composition effect of more old workers that have very high part-time rates.

Median potential output and possible labor volume development

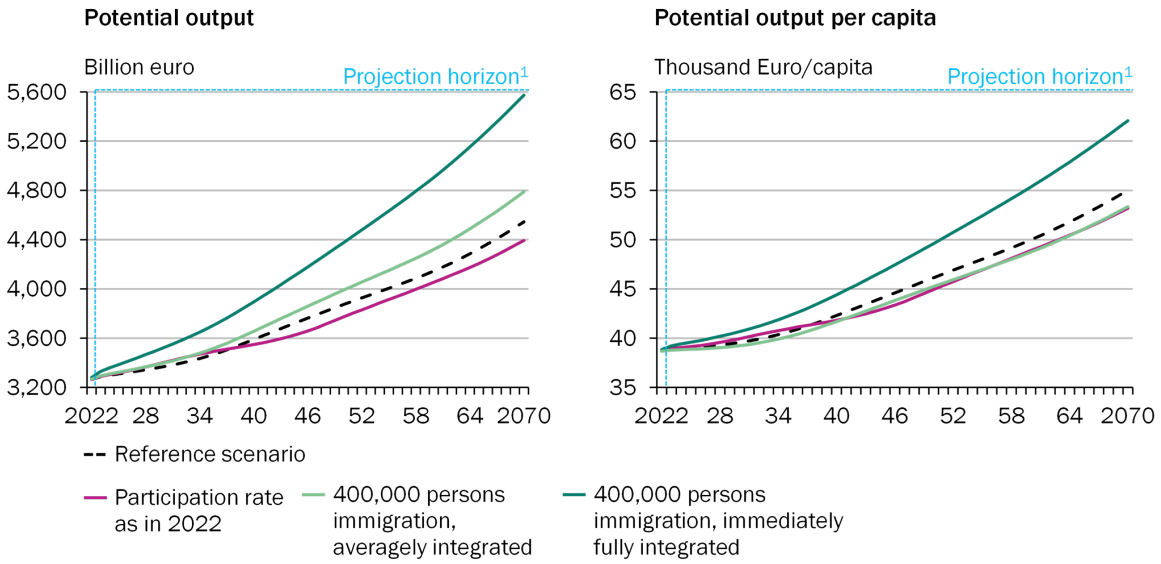

1 – Values for the years 2023 and 2024 are based on the short-term forecast by the GCEE. From 2025 projection.

Sources: Federal Statistical Office, IAB, OECD, own calculations

Figure 10

To illustrate the model's capability in quantitatively assessing such considerations, we prioritize the second strategy, which is more feasible to implement. In this context, we delve into potential risks and opportunities for labor volume growth, all of which can be influenced by well-crafted policies to varying degrees of (im)probability. For instance, as depicted in Figure 10, if the anticipated rise in the labor participation rate to 75% is not realized and remains at the current 69% (violet line), the median potential output per capita in 2070 would decline by 3% compared to the baseline projection (black dashed line).

In contrast, as illustrated in Figure 10, a higher net migration of around 400,000 individuals annually (light green line), as opposed to the assumed 250,000, could potentially raise output by about 5% in 2070. However, given our assumption of weaker integration of immigrants[12] into the German labor market, potential output per capita might decrease by 3% compared to the baseline projection.[13]

[12] We assume they have a labor participation rate of 70%, as the native population, but a structural unemployment rate of 12%.

[13] As a theoretical alternative, if net migration comprised 400,000 individuals immediately and fully integrated into the labor market (i.e., with zero unemployment rates and 100% labor participation; dark green line), potential output would be 22% higher, with per capita potential output in 2070 being 13% above the baseline projection. This represents only the direct effect on potential output. Additionally, an increase in innovative activity may enhance the proportion of highly qualified individuals, potentially leading to a more significant improvement in total factor productivity (TFP) and, consequently, potential output.

7 Conclusion

We explored the interaction between demographic dynamics and Germany's potential output dating back to 1970 using a Bayesian approach and the Cobb-Douglas production function. Leveraging Bayesian techniques and a robust stochastic volatility framework, we achieved precise estimation. Moreover, our methodology's exceptional stability over extended time periods allowed us to perform potential output projections up to 2070 and to assess the quantitative impact of policy strategies.

Our long-term projections conditional on current economic dynamics imply that future, anticipated demographic changes will exacerbate the decline of potential output growth, with median growth rates projected to average around 0.4% throughout the 2020s. While these projections are informative on their own, more importantly, they help to inform policy makers with long-term objectives. For instance, long-term economic growth paths are crucial for pension and health system design, fiscal budget planning or social security reforms. They can also help investors make capital allocation decisions.

Several factors have contributed to Germany's declining potential growth since 1970. While a major factor in the long-run is the slowdown in total factor productivity growth, the primary driver of recent growth declines, particularly since 2018, has been the shrinking labor volume in Germany, even before the pandemic. In addition, our simulations indicate that shocks in the context of the labor market during both the pandemic and the recent energy crisis have permanently affected Germany's growth prospects. While demography alone may not be blamed for the past reductions of the labor volume – to a large extent, this appears to be caused by very widespread adoption of part-time work arrangements – demography is with very high probability the main determinant of future labor volume reductions.

There are several promising avenues for future model enhancements. One significant advancement could involve partially endogenizing total factor productivity projections by incorporating connections with human capital and labor input. Moreover, additional model components can be considered, e.g. related to social security or the fiscal balance. Furthermore, some components of the model, such as human capital, hours or labor participation, may benefit from even more disaggregation to track demographic transmission even better. Finally, examining pseudo-revisions over longer horizons or even on real-time data could provide valuable insights into the model's long-term performance.

References

Acemoglu, D. (2006): "A Simple Model of Inefficient Institutions," *The Scandinavian Journal of Economics*, 108, 515–546.

Aikman, D., M. Drehmann, M. Juselius, and X. Xing (2022): "The scarring effects of deep contractions," Working Paper 1043, BIS.

Anger, C., A. Plünnecke, and J. Schmidt (2010): "Bildungsrenditen in Deutschland: Einflussfaktoren, politische Optionen und ökonomische Effekte," *IW-Analysen*, 65.

Barro, R. and X. Sala-i Martin (1991): "Convergence across States and Regions," *Brookings Papers on Economic Activity*, 22, 107–182.

——— (1997): "Technological Diffusion, Convergence, and Growth," *Journal of Economic Growth*, 2, 1–26.

Barro, R. J. (2015): "Convergence and Modernisation," *The Economic Journal*, 125, 911–942.

Belzile, L. (2020): "TruncatedNormal," R-package.

Berger, T., G. Everaert, and H. Vierke (2016): "Testing for time variation in an unobserved components model for the U.S. economy," *Journal of Economic Dynamics and Control*, 69, 179–208.

Berger, T. and B. Kempa (2019): "Testing for time variation in the natural rate of interest," *Journal of Applied Econometrics*, 34, 836–842.

Berger, T. and C. Ochsner (2022): "Robust Real-Time Estimates of the German Output Gap based on a Multivariate Trend-Cycle Decomposition," Bundesbank Discussion Paper 35/2022.

Blanchard, O. J. and L. H. Summers (1986): "Hysteresis and the European unemployment problem," *NBER Macroeconomics Annual*, 1, 15–78.

——— (1987): "Hysteresis in unemployment," *European Economic Review*, 31, 288–295.

Bloom, N., C. I. Jones, J. Van Reenen, and M. Webb (2020): "Are Ideas Getting Harder to Find?" *American Economic Review*, 110, 1104–44.

Botev, Z. I. (2017): "The normal law under linear restrictions: simulation and estimation via minimax tilting," *Journal of the Royal Statistical Society: Series B (Statistical Methodology)*, 79, 125–148.

Breuer, S. and S. Elstner (2020): "Germany's Growth Prospects against the Backdrop of Demographic Change," *Journal of Economics and Statistics*, 240, 565–605.

Brueggemann, R., C. Jentsch, and C. Trenkler (2016): "Inference in vars with conditional heteroskedasticity of unknown form," *Journal of Econometrics*, 69–85.

CBO (1995): "CBO's Method for Estimating Potential Output," .

Cerra, V., A. Fatas, and S. C. Saxena (2023): "Hysteresis and Business Cycles," *Journal of Economic Literature*, 61, 181–225.

Chalaux, T. and Y. Guillemette (2019): "The OECD Potential Output Estimation Methodology," *Economics Department Working Paper*.

Chan, J. and I. Jeliazkov (2009): "Efficient simulation and integrated likelihood estimation in state space models," *International Journal of Mathematical Modelling and Numerical Optimisation*, 101–120.

Chan, J., G. Koop, D. J. Poirier, and J. L. Tobias (2019): "Bayesian econometric methods," Tech. rep.

Chan, J., G. Koop, and S. Potter (2013): "A New Model of Trend Inflation," *Journal of Business Economic Statistics*, 31, 94–106.

Chan, J. C. and E. Wemy (2023): "An unobserved components model of total factor productivity and the relative price of investment," *Macroeconomic Dynamics*, 27, 1397–1423.

Chan, J. C. C., G. Koop, and S. M. Potter (2016): "A Bounded Model of Time Variation in Trend Inflation, Nairu and the Phillips Curve," *Journal of Applied Econometrics*, 31, 551–565.

Chib, S. and E. Greenberg (1994): "Bayes inference in regression models with ARMA (p, q) errors," *Journal of Econometrics*, 64, 183–206.

de la Fuente, A. and R. Doménech (2006): "Human Capital in Growth Regressions: How Much Difference Does Data Quality Make?" *Journal of the European Economic Association*, 4, 1–36.

Fatás, A. (2000): "Endogenous growth and stochastic trends," *Journal of Monetary Economics*, 45, 107–128.

Gali, J. (2015): *Monetary Policy, Inflation, and the Business Cycle: An Introduction to the New Keynesian Framework and Its Applications*.

Galor, O. (2011): *Unified Growth Theory*, Princeton University Press.

German Council of Economic Experts (2022): *Managing the energy crisis in solidarity and shaping the new reality*.

——— (2023): *Strengthening potential output through investment and innovation*.

Goldin, I., P. Koutroumpis, F. Lafond, and J. Winkler (forthcoming): "Why Is Productivity Slowing Down?" .

Gopinath, G., Kalemli-Özcan, L. Karabarbounis, and C. Villegas-Sanchez (2017): "Capital Allocation and Productivity in South Europe*," *The Quarterly Journal of Economics*, 132, 1915–1967.

Gordon, R. J. (2012): "Is U.S. Economic Growth Over? Faltering Innovation Confronts the Six Headwinds," Working Paper 18315, National Bureau of Economic Research.

Grant, A. L. and J. C. Chan (2017a): "A Bayesian Model Comparison for Trend-Cycle Decompositions of Output," *Journal of Money, Credit and Banking*, 49, 525–552.

——— (2017b): "Reconciling output gaps: Unobserved components model and Hodrick–Prescott filter," *Journal of Economic Dynamics and Control*, 75, 114–121.

Hamilton, J. D. (2018): "Why You Should Never Use the Hodrick-Prescott Filter," *The Review of Economics and Statistics*, 100, 831–843.

Havik, K., K. McMorrow, F. Orlandi, C. Planas, R. Raciborski, W. Roeger, A. Rossi, A. Thum-Thysena, and V. Vandermeulen (2014): "The Production Function Methodology for Calculating Potential Growth Rates Output Gaps," *Economic Papers*.

Hochmuth, B., B. Kohlbrecher, C. Merkl, and H. Gartner (2021): "Hartz IV and the decline of German unemployment: A macroeconomic evaluation," *Journal of Economic Dynamics and Control*, 127, 104114.

Hodrick, R. J. and E. C. Prescott (1997): "Postwar U.S. Business Cycles: An Empirical Investigation," *Journal of Money, Credit and Banking*, 1–16.

Kim, C.-J. and C. R. Nelson (1999): *State-space models with regime switching. Classical and Gibbs-sampling approaches with applications*, MIT Press.

Kim, S., N. Shephard, and S. Chib (1998): "Stochastic Volatility: Likelihood Inference and Comparison with ARCH Models," *The Review of Economic Studies*, 65, 361–393.

Knetsch, T. A. (2013): "A User Cost Approach to Capital Measurement in Aggregate Production Functions," *Jahrbücher für Nationalökonomie und Statistik*, 233, 638–660.

Kotschy, R. and D. E. Bloom (2023): "Population Aging and Economic Growth: From Demographic Dividend to Demographic Drag?" Working Paper 31585, National Bureau of Economic Research.

Mankiw, N. G., D. Romer, and D. N. Weil (1992): "A Contribution to the Empirics of Economic Growth*," *The Quarterly Journal of Economics*, 107, 407–437.

Mertens, E. (2023): "Precision-based sampling for state space models that have no measurement error," *Bundesbank Discussion paper*.

Morley, J. and B. Wong (2020): "Estimating and accounting for the output gap with large Bayesian vector autoregressions," *Journal of Applied Econometrics*, 35, 1–18.

Morley, J. C., C. R. Nelson, and E. Zivot (2003): "Why Are the Beveridge-Nelson and Unobserved-Components Decompositions of GDP So Different?" *The Review of Economics and Statistics*, 85, 235–243.

Müller, U. K., J. H. Stock, and M. W. Watson (2022): "An Econometric Model of International Growth Dynamics for Long-Horizon Forecasting," *The Review of Economics and Statistics*, 104, 857–876.

Müller, U. K. and M. W. Watson (2016): "Measuring Uncertainty about Long-Run Predictions," *The Review of Economic Studies*, 83, 1711–1740.

Ochsner, C. (forthcoming): "Bayesian Time Series Simulation, Estimation and Prediction of Trend-Cycle Decompositions and ARMAX(p,q,n) processes with stochastic volatility and time-varying parameters in `R`," .

OECD (2009): *Measuring Capital. OECD Manual*.

Orphanides, A. and S. van Norden (2002): "The Unreliability of Output-Gap Estimates in Real Time," *The Review of Economics and Statistics*, 84, 569–583.

Pfeiffer, F. and H. Stichnoth (2021): "Fiscal and individual rates of return to university education with and without graduation," *Applied Economics Letters*, 28, 1432–1435.

Quast, J. and M. H. Wolters (2022): "Reliable real-time output gap estimates based on a modified Hamilton filter," Tech. rep.

Ramsey, F. P. (1928): "A Mathematical Theory of Saving," *The Economic Journal*, 38, 543–559.

Restuccia, D. and R. Rogerson (2008): "Policy distortions and aggregate productivity with heterogeneous establishments," *Review of Economic Dynamics*, 11, 707–720.

——— (2017): "The Causes and Costs of Misallocation," *Journal of Economic Perspectives*, 31, 151–74.

Romer, P. M. (1986): "Increasing Returns and Long-Run Growth," *Journal of Political Economy*, 94, 1002–1037.

Schmalwasser, O. and M. Schidlowski (2006): "Measuring Capital Stock in Germany," *Wirtschaft und Statistik*.

Shackleton, R. (2018): "Estimating and Projecting Potential Output Using CBO's Forecasting Growth Model," *Working paper*.

Smets, F. and R. Wouters (2007): "Shocks and frictions in US business cycles. A bayesian DSGE approach," *American Economic Review*, 97, 586–606.

Solow, R. (1956): "A Contribution to the Theory of Economic Growth," *Quarterly Journal of Economics*, 70, 65–94.

Walsh, C. E. (2017): *Monetary Theory and Policy*.

Wanger, S. (2023): "Erwerbstätigkeit, Arbeitszeit und Arbeitsvolumen von Frauen und Männern: Entwicklungen seit der Covid-19-Pandemie." *IAB-Forschungsbericht*, 18/2023, 543–559.

A Some Remarks

The outcome of our analysis results in a random sample for potential output, potential output growth, and the output gap. The distributions of the samples of these aggregated series are not straightforwardly attributable to common statistical families. This is a notable difference to the case where potential was estimated from GDP directly (e.g. by applying the filter outlined in Appendix G). To get an idea of their distributions, note that, e.g. in case of potential output, we have

$$\begin{aligned} \overline{y}_t &= y_t - \widetilde{y}_t \\ \text{then, by Eq. (1)} & \\ &= \overline{a}_t \times (\overline{hl}_t)^{\alpha} \times (\overline{k}_t)^{(1-\alpha)} \\ &= \overline{(y_t - (h_t(b_t w_t(1-u_t)s_t))^{\alpha} \times k_t^{(1-\alpha)})} \\ &\quad \times (\overline{h}_t(b_t\overline{w_t}(1-\overline{u_t})\overline{s_t}))^{\alpha} \\ &\quad \times (\overline{k}_t)^{(1-\alpha)} \end{aligned} \tag{21}$$

where the right-hand side expression is a composite of various samples. Note that for J retained draws, $\hat{\bar{\boldsymbol{y}}} = \frac{1}{J}\sum_{i=1}^{J} \bar{\boldsymbol{y}}^j$ and $\hat{\boldsymbol{\Sigma}}^{\bar{y}} = \frac{1}{J-1}(\bar{\boldsymbol{y}}^j - \hat{\bar{\boldsymbol{y}}})(\bar{\boldsymbol{y}}^j - \hat{\bar{\boldsymbol{y}}})'$ are unbiased estimators of the mean and covariance of potential output. Now assume that the resulting sample is multivariate normal distributed: Most of the right-hand side terms have normal or log-normal posteriors and thus constitute normal and log-normal random samples. In addition, the product of log-normal samples is known to be log-normal as well and the sums of normal samples obey a normal distribution. It is known that log-normal distributions converge towards normal distributions if their volatility approaches zero (trends, by definition, have very small volatilities, see the Technical Appendix). Therefore, we can regard the right-hand side as approximately normal.

Figure 11 compares the fifth, fiftieth and ninety-fifth quantiles of the resulting normal (orange) with the respective quantiles of our sample (blue) for potential output (left panel) and the output gap (right panel). In fact, both match very well. This underlines that our disaggregated approach yields a very reasonable approximation to a normal posterior of potential output that would, for example, emerge from filtering gross domestic product directly under the assumption of normality. However, our approach generates much additional information compared to a simple decomposition of GDP.

Model-implied estimate of potential output growth and output gap vs. normal distribution

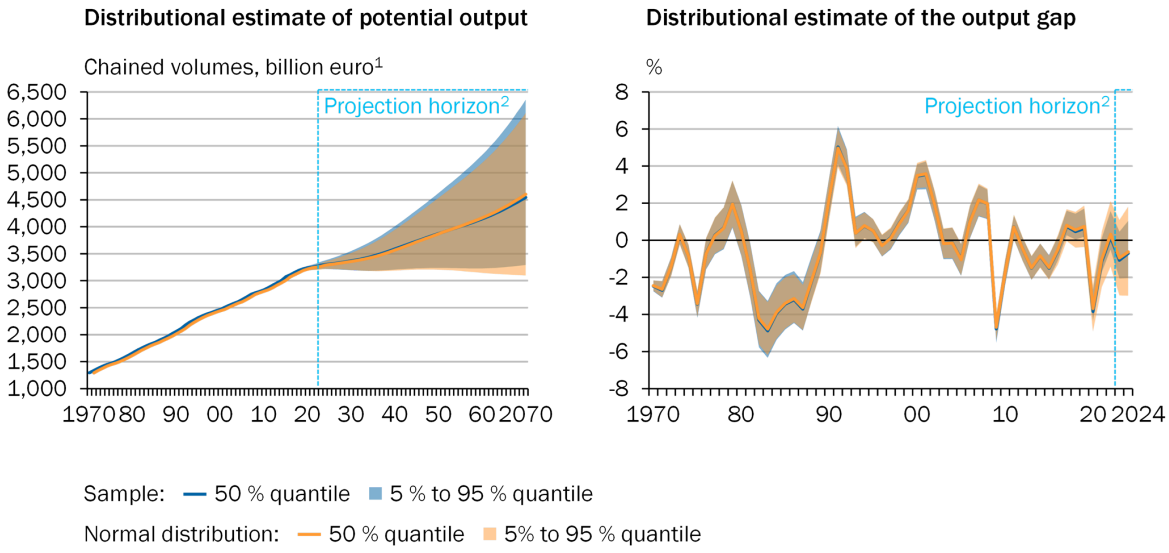

1 – Reference year 2015. 2 – Values for 2023 and 2024 are based on the German Council of Economic Experts' short-term forecast. From 2025 projection, results of the reference scenario.

Sources: Federal Statistical Office, IAB, OECD, own calculations
© Sachverständigenrat | 23-463-01

Figure 11

B Labor Volume and Human Capital

Total hours work derive from the population in the working age (henceforth population), labor participation, the structural unemployment rate and the average hours worked. Figure 12 shows trend growth and gap components for the labor aggregates. Note that in the case of aggregate labor participation, we observe a notable composition effect in the 2040s (third row, first column), as the age groups with higher participation rates become relatively larger in the working age population.

Labor Aggregates

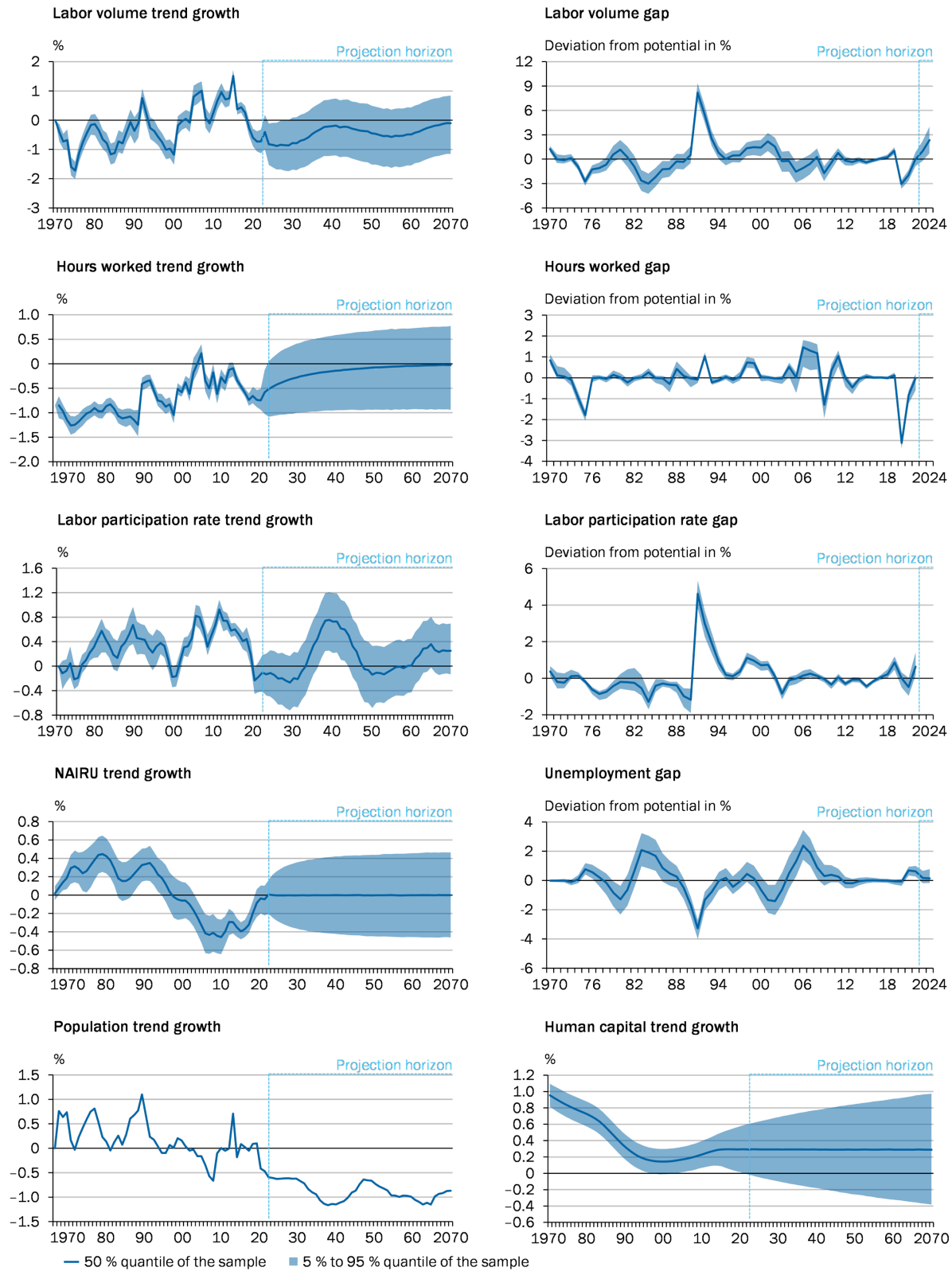

Sources: Federal Statistical Office, IAB, OECD, own calculations
© Sachverständigenrat | 23-210-01

Figure 12

C Capital Services

The required return to capital is shown in Figure 13 and capital service composition is shown in Figure 14.

Required rate of return to capital

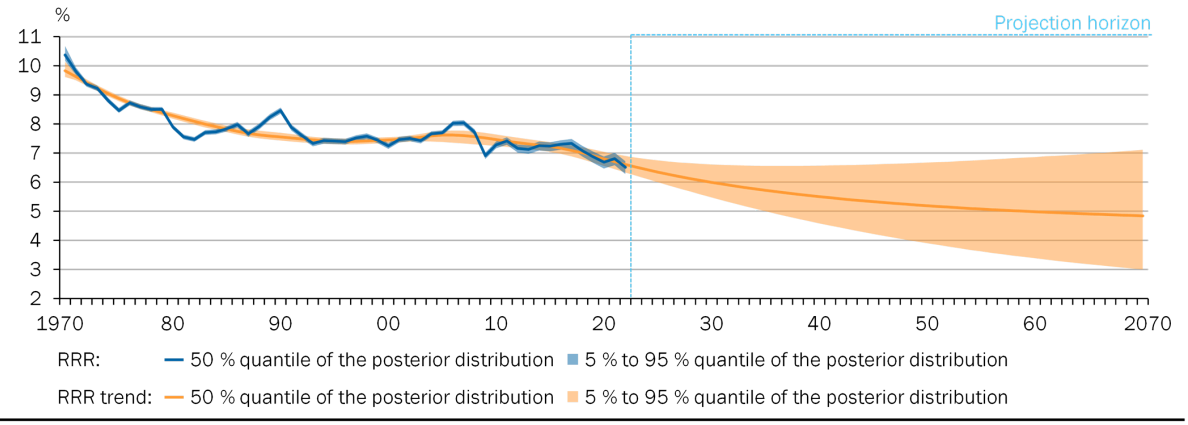

Sources: Federal Statistical Office, own calculations
© Sachverständigenrat | 23-369-01

Figure 13

Shares in capital use and capital costs of different capital goods

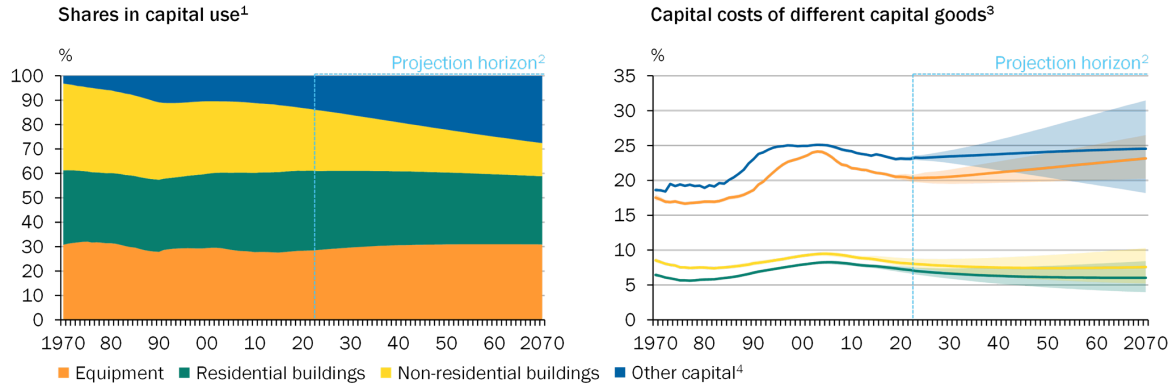

1 – 50 % quantil of the sample is shown. 2 – Values for 2023 and 2024 are based on the short-term forecast by the GCEE. From 2025 projection, results of the reference scenario. 3 – The solid line corresponds to the 50 % quantile, the areas to the 5 % to 95 % quantile of the sample.
4 – Mainly Intellectual Property.

Sources: Federal Statistical Office, own calculations
© Sachverständigenrat | 23-168-02

Figure 14

Figure 15 shows depreciation and disposal volumes computed from the investment projections for the entire investment projection distribution.

Depreciation and disposal volumes by capital good

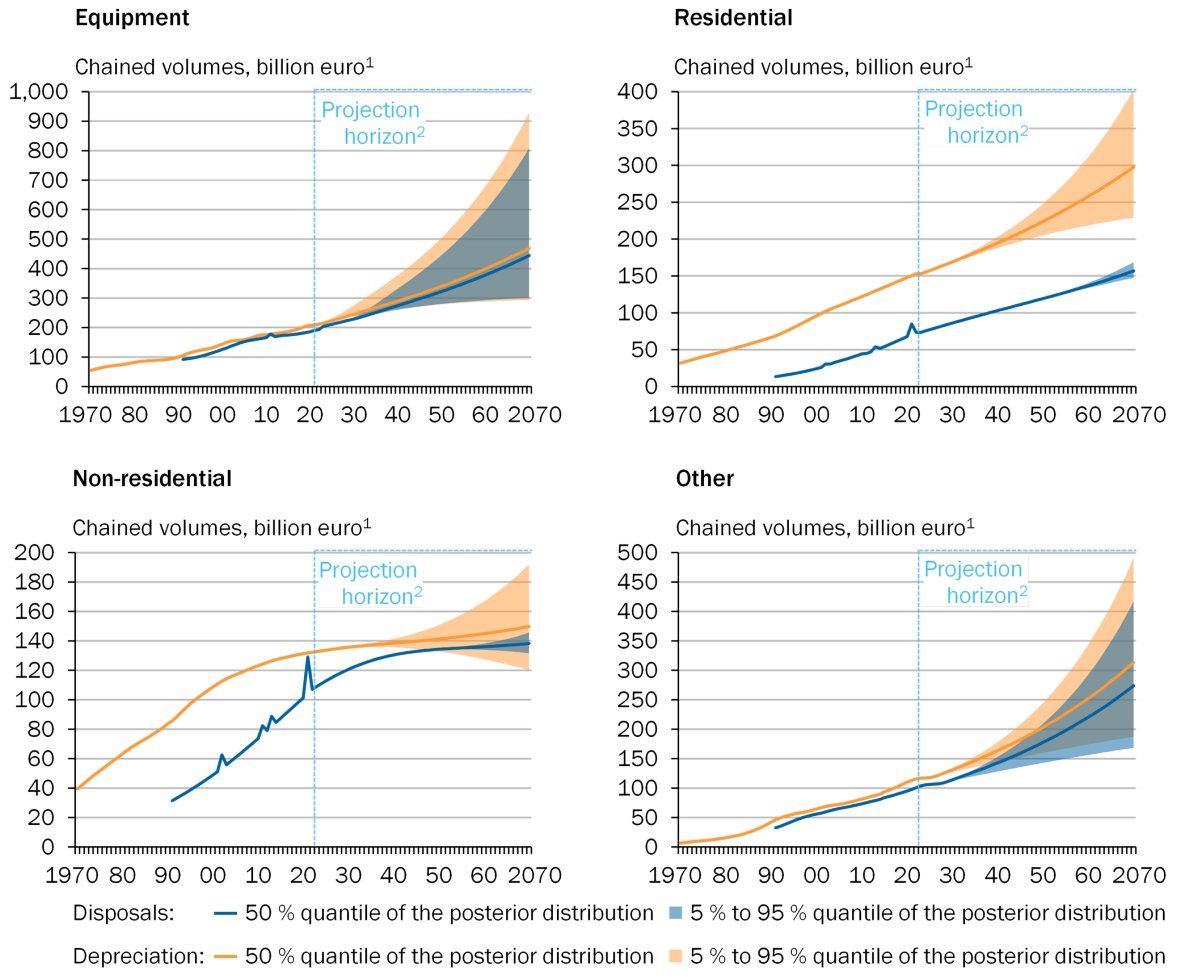

1 – Reference year 2015. 2 – Values for 2023 and 2024 are based on the German Council of Economic Experts' short-term forecast. From 2025 projection, results of the reference scenario.

Sources: Federal Statistical Office, own calculations

Figure 15 Disposal and depreciation volumes for each capital good in billions of chained 2015 euros.

D Analysis of Backward and Forward Revisions

In this appendix, we conduct a retrospective analysis of revisions made to potential output, potential output growth, and the output gap.

D.1 The Role of Unanticipated Shocks to Trend Growth

The long-term forecasts fundamentally depend on the component-specific trend growth forecasts (see Section 3). Recall that, while our approach allows us to project trend and cycle of all components into the future, we take the population projection from the Federal Statistical Office. Consequently, our model fully anticipates future population dynamics. In contrast, new incoming data for the model's remaining components may lead to a revision of the adjustment path to long-run trend growth. Downward deviations from long-run trend growth will lead to sluggish adjustment in the model's dynamics, deteriorating the long-run growth outlook. Economically, changes in trend growth can be caused by i) shocks to deep parameters such as preferences or ii) output hysteresis, which occurs when an economy operates below its full capacity for a long time, e.g. due to (a series of) contractionary demand shocks causing lasting damage to its ability to produce efficiently (Blanchard and Summers 1986, 1987, Aikman et al. 2022, Cerra et al. 2023).

To investigate how much unanticipated changes in trend growth not related to population dynamics have led to the current dim growth outlook, we take advantage of the model's foresight about population dynamics. We conduct several runs of our model starting from 2018.[14] Each time, we introduce a new piece of information for the following year $(t+1)$. For example, when computing the 2018 pseudo-vintage, we only use data up to 2017 and project from there. We do not use real-time data vintages.[15] This setup ensures that the model conditions upon (anticipated) changes in demographics across all the simulated vintages. As a result, any alteration in potential output from one simulated period in year t to the next one in year $t+1$ happens only because of shocks to trend growth. This analysis helps us to figure out if the sluggish growth forecast is to due to exogenous changes, indicating a clear link to demographic shifts in case trend growth revisions are small, or if they stem from unexpected shifts in fundamentals as e.g. worker's preferences, leading to larger trend growth revisions.

Figure 16 illustrates the results of our experiment, clearly showing a substantial deterioration in Germany's economic growth outlook since 2018 (upper left panel). In fact, whereas the average projected potential output growth rate until 2070 is 1.2 % in the 2018-model-vintage (when the model is unconscious of COVID-19 and the energy crisis, but foreseeing reduced labor force and participation rate effects of demographic shifts), it deteriorated to 0.7 % in the 2023-model vintage. While we see moderate downward revisions in capital services and TFP (second column), the largest downward revision clearly results from total working hours (lower left panel, first column), even when we

[14] Each pseudo-vintage incorporates a pseudo-business cycle forecast for the next year, e.g. in 2018 for 2019. Thus, starting this exercise in 2018 provides a simple counterfactual scenario free of any pandemic effects.

[15] By avoiding real-time data and forecasts, our model remains largely unaffected by short-term prediction errors. Importantly, historical revisions are minimized, except for random sampling errors.

control for the projected demographic developments. Therefore, we investigate whether trend growth deteriorations in labor market aggregates (other than population dynamics) explain the downward adjustment of potential labor volume between 2018 and 2023.

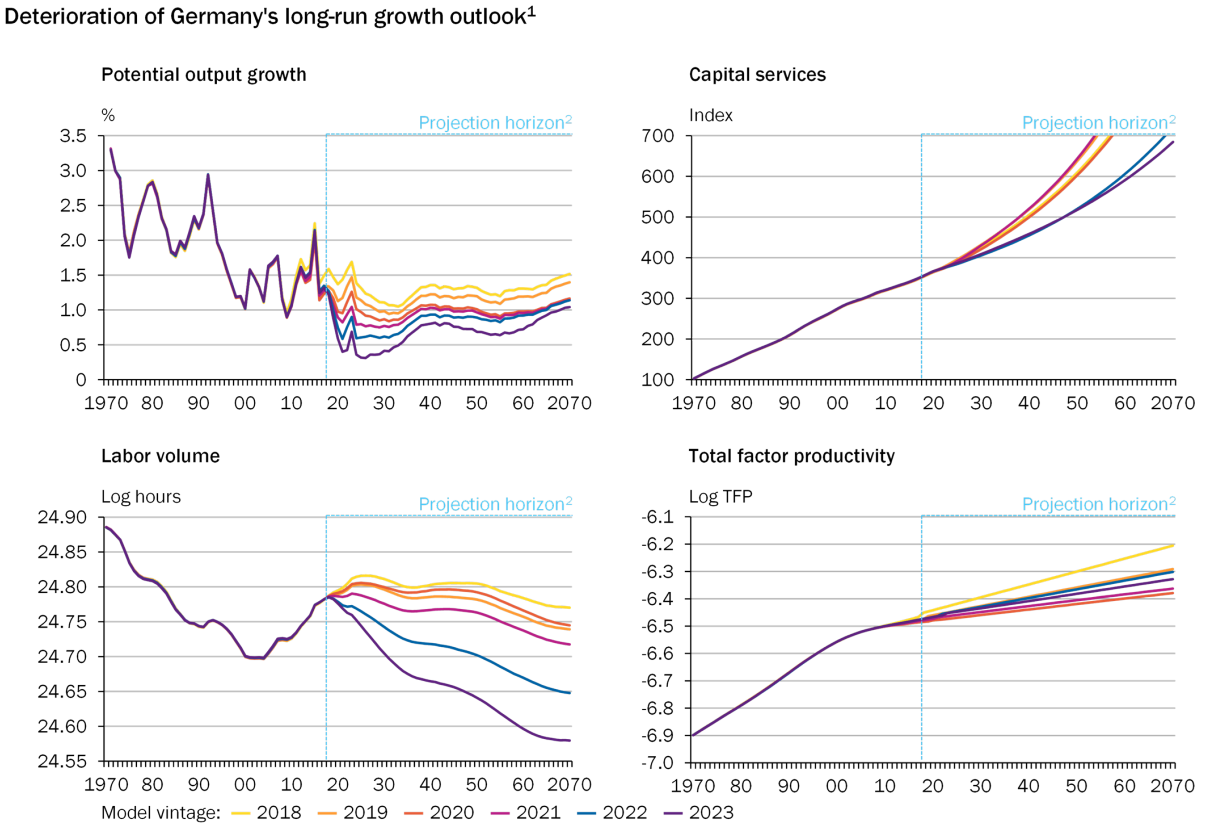

Figure 16

Figure 17 shows the deterioration in trend (growth) of working hours by full-time workers, one of the most important factors for the deterioration of the labor market outlook (left panel). The median trend growth rate has decreased from -0.05% in 2015 to -0.75% in 2023, as indicated by the solid purple lines (right panel). It is important to emphasize that the trend growth of full-time working hours reverts to its mean (zero) over time, as explained in Section 3. However, real-world data consistently deviates from the model-implied expectations, resulting in repeated downward adjustments of trend growth and subsequently, revisions of the adjustment path to the mean.

It is crucial to note that even if full-time working hours swiftly reverted to their pre-pandemic levels, potentially leading to an upward revision of the trend, they would likely still remain below historical averages. This lends support to the hypothesis that the model correctly detects a permanent deterioration of the trend growth of working hours that is not exclusively linked to pandemic events. Such a deviation from historical norms would continue to impact the overall growth outlook negatively compared to levels seen in 2018 or earlier.

Revisions of full-time hours worked[1]

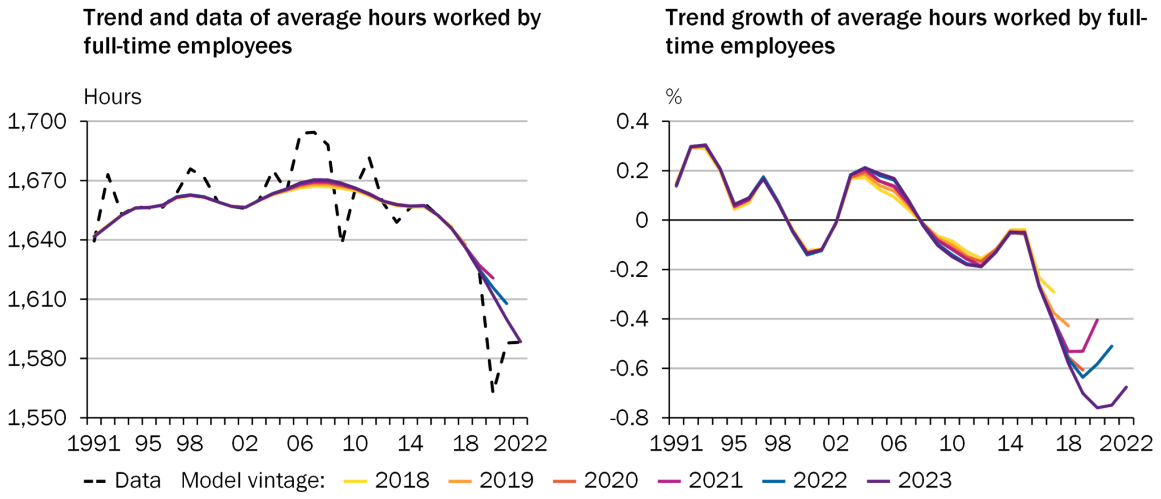

1 – Depicted are the sample medians.

Sources: IAB, own calculations

Figure 17

Identifying the causes behind the decrease in full-time working hours presents a more intricate challenge. It might seem convenient to attribute the entire decline to the COVID-19 pandemic, yet this oversimplifies the situation. The downturn in trend growth for full-time working hours began much earlier, around 2015 (refer to Figure 17, upper left panel), hinting that non-crisis-related factors could be contributing to this downward trend. Possible contributors to this decline include the reduction in overtime work (dropping from an average of 22 overtime hours per worker in 2015 to 14 in 2022) and an upsurge in sick leave hours (from 60 hours per worker annually in 2015 to 91 hours per worker in 2022). A basic estimation suggests that even considering both factors, full-time working hours in 2022 would have been only 2 percentage points higher, which is merely half of the difference (4%) between full-time working hours in 2015 and 2022.[16]

As innovations to working hours do not have a structural interpretation in our modeling framework, explaining the remaining half of the level shift in working hours, is not straightforward. As for labor force and labor participation (see Figure 4), the projected demographic transition may be a factor, with part-time rates being presumably high among elderly workers. Recall that the model is agnostic regarding demography as a critical factor influencing working hours. The causal link between demography and hours outlined in Section 5.1 is essential to this.

[16]It is worth noting that changes in *observed* full-time working hours (see Figure 17, first column, first row, dashed black line) during the pandemic may correlate with changes in 'Kurzarbeit' hours (a policy for times of economic stress designed to reduce hours and avoid layoffs through government wage support), but these are likely absorbed into the cyclical component during the filtering process (see the Technical Appendix) and may not explain the decline in hours.

D.2 Backward Revisions

Building upon the experiment detailed in Section D.1, we present a comparison of overall revisions. Our data vintages are pseudo-real-time and the sample is limited by data availability. The second column specifically focuses on revisions for the year 2018 between the nowcast with the 2018 data and estimation vintage and the backcast with the most recent 2023 vintage. Remarkably, our experiment reveals that potential output undergoes minimal revisions over the entire estimation period, with an average revision rate of just -0.14%. Furthermore, the model provides estimates for potential output growth and the output gap spanning five decades that show a high degree of consistency across various vintages, on average. Notably, neither cyclical nor anti-cyclical revisions appear to dominate in our analysis.

	Average 1970 - 2018	2018
Potential Output Revision in %	-0.137	1.334
Difference Potential Output Growth	0.003	0.567
Difference Output Gap	0.133	-1.330

Table 3 Revisions of potential output estimates. First column reports the time-average of overall revisions between the 2018 pseudo-real-time model vintage and the 2023 vintage. Second column reports the revisions for the year 2018 for both vintages.

Nonetheless, it is important to emphasize the relatively substantial revisions to potential output estimated with data up to 2023 compared to 2018, as indicated in the second column of Table 3. Note that Figure 18 provides the full picture.While the level of potential output experiences a 1% revision (equivalent to approximately 32 billion euros), a significant portion of the revision is retrospectively shifted from potential output growth to the output gap. This outcome is a natural consequence of Bayesian updating. As time passes, the model incorporates more data. From the model's perspective, what initially appeared to be a temporary under-utilization of capacity evolves into a substantial deterioration of the long-term growth outlook (see Section 5).

To illustrate this, consider the estimated median of trend growth in full-time employee working hours for the year 2018. In the 2018 vintage, this median is calculated as -0.27, with the corresponding cyclical component at -0.11. However, in the 2023 vintage, while the cyclical component for 2018 is close to zero (0.01), trend growth has deteriorated significantly to -0.41. It is crucial to stress that this updating behavior is not a flaw but a deliberate and a desirable characteristic of the model. Unless economic deteriorations prove to be persistent, regardless of their magnitude, they are absorbed into the cyclical component. This leads to stable estimates of potential output levels over time, on average. In contrast, it is well recognized that the Hodrick and Prescott (1997) filter can produce misleading signals when confronted with large but potentially transitory fluctuations (as during COVID-19) in data (Hamilton 2018). Consequently, production-function models relying on this or similar filters, as regularly used by policy institutions to disentangle trends and cycles, may be susceptible to such shortcomings as well.

Finally, we emphasize that different models serve different purposes. In light of our find-

ings, it becomes evident that for real-time assessments of the output gap, specialized nowcasting procedures, such as the one proposed by Berger and Ochsner (2022) for Germany, are better suited to provide timely and accurate information to policy makers. However, it is worth noting that from a policy perspective, these multivariate models do have limitations in that they lack the (semi-)structural interpretation that a production-function model offers. Therefore, when assessing the structural development of an economy, the latter proves to be superior.

Percentage revisions of potential output[1]
Revisions in % of a given vintage compared to the previous vintage

	Model Vintage					Average (all vintages)
	2018	2019	2020	2021	2022	
Potential						
Average (1970 – 2017)	– 0.16	– 0.04	0.04	0.03	0.01	– 0.03
2018	– 1.33	– 0.83	0.48	0.45	– 0.08	– 0.26
2019	– 1.52	– 0.95	0.39	0.36	– 0.18	– 0.38
2020	– 1.76	– 1.09	0.29	0.21	– 0.34	– 0.54
2021	– 2.00	– 1.30	0.15	– 0.02	– 0.53	– 0.74
2022	– 2.23	– 1.52	– 0.04	– 0.21	– 0.87	– 0.97
2023	– 2.44	– 1.72	– 0.25	– 0.36	– 1.07	– 1.17
TFP						
Average (1970 – 2017)	– 0.14	– 0.05	0.00	0.04	0.01	– 0.03
2018	– 2.29	– 1.05	0.59	0.55	– 0.03	– 0.44
2019	– 1.71	– 1.94	0.70	0.62	– 0.02	– 0.47
2020	– 1.83	– 1.85	0.50	0.73	– 0.03	– 0.49
2021	– 1.96	– 2.03	0.91	0.50	– 0.01	– 0.52
2022	– 2.09	– 2.20	0.98	1.18	– 0.60	– 0.54
2023	– 2.21	– 2.34	1.01	1.26	– 0.13	– 0.48
Capital Services						
Average (1970 – 2017)	0.36	– 0.38	0.38	0.00	0.00	0.07
2018	0.58	– 0.46	0.46	– 0.01	0.02	0.12
2019	0.69	– 0.48	0.45	– 0.01	0.03	0.14
2020	0.63	– 0.53	0.49	– 0.01	0.04	0.12
2021	0.34	– 0.62	0.59	– 0.13	0.05	0.05
2022	0.26	– 0.93	0.63	– 0.29	0.11	– 0.05
2023	0.38	– 1.28	0.42	– 0.45	0.34	– 0.12
Labour						
Average (1970 – 2017)	0.01	– 0.03	0.03	0.00	0.01	0.00
2018	– 0.15	0.12	– 0.08	– 0.11	– 0.01	– 0.05
2019	– 0.31	0.13	– 0.30	– 0.39	– 0.09	– 0.19
2020	– 0.52	0.19	– 0.51	– 0.76	– 0.26	– 0.37
2021	– 0.69	0.21	– 0.80	– 1.21	– 0.46	– 0.59
2022	– 0.85	0.23	– 1.10	– 1.53	– 0.89	– 0.83
2023	– 1.01	0.23	– 1.35	– 1.78	– 1.27	– 1.04

1 – Blue fields are backward looking, orange fields incorporate at least one forecast.

Sources: Federal Statistical Office, IAB, OECD, own calculations

Figure 18

D.3 Scars from Recent Economic Turmoil

The beginning of the new decade brought about a confluence of challenges for the German economy, with the impacts of the COVID-19 pandemic and the concurrent energy crisis significantly depressing investment trends. The persistence of the pandemic, particularly with the emergence of new variants, continued to disrupt global supply chains and hamper economic activities. The energy crisis of 2022, characterized by surging energy prices as well as the monetary policy response to high inflation further exacerbated the economic challenges faced by the German economy (German Council of Economic Experts 2022). In particular, the spike in energy costs placed additional strains on businesses, especially those in energy-intensive sectors.

Against this backdrop, it is unsurprising that not only the labor input deteriorates since our first model pseudo-vintage (2018), but so do capital services and TFP (see Figure 16). Whereas the forecast revisions of TFP do not exhibit a systematic pattern, this is different for capital services. While projected capital services experience only minor forecast revisions until the pseudo-2021-vintage, we observe downward revision in the pseudo-2022-vintage. This revision is primarily attributed to the decline in equipment investment trend growth, that was revised downward from 2.5% annual in 2021 to 1.5% annual in 2022. This shift in projections allows for the potential influence of output hysteresis, e.g. via deteriorated expectations of future returns. For instance, Fatás (2000) shows that in an endogenous growth model transitory disturbances, e.g., because of an uncertainty shock, can result in persistent effects for capital accumulation. Similarly, limited investment-financing due to the current monetary policy stance manifests in smaller trend growth for equipment investments and, thus, may affect capital accumulation permanently.

E Output Gap

Actual GDP fluctuates around potential output. The deviation between both measures is the 'output gap' and defined as the difference between actual GDP and potential output expressed in percent of potential output. Examining the output gap and comparing it to established estimates may also help clarify the quality of our results. A closed output gap, where actual GDP equals potential output, serves as an indicator of economic stability and efficiency. A positive output gap signals overheating and the possibility of rising inflation. According to standard business cycle theory, this can result in inflationary pressures, prompting central banks to contemplate raising interest rates to temper economic activity (Gali 2015, Walsh 2017). In response, central banks raise interest rates to dampen demand. Conversely, when the actual GDP falls short of the potential output, resources are underutilized. Due to low demand, firms lay off employees which leads to higher unemployment. To increase economic activity, policymakers may implement expansionary measures to close the output gap.

Figure 19 illustrates the output gap as implied by our model.[17] The output gap exhibits a cyclical pattern with a zero mean by design. It typically turns negative during economic recessions, as identified by the German Council of Economic Experts (e.g. 2017, 2021, 2022). Subsequently, it recovers over time. One of the most significant downturns, reaching as low as -4.8%, occurred during the recession in the early 1980s during the second oil crisis.

To investigate the determinants of the output gap, we decompose it into contributions that result from the TFP gap and the labor volume gap. Note that the model is in reduced form such that the decomposition does not allow for a causal interpretation. However, the decomposition sheds light onto the question whether the underlying structural shocks transmit through TFP or the labor market. The TFP gap measured as the difference between the Solow residuum and the trend aligns quite close with most of the German economy recessions documented by the GCEE. Clearly, the output gap is mostly driven by TFP-inefficiencies. Note that TFP measures technical as well as (factor-)allocative efficiency, where in broad terms, allocative inefficiencies should be transitory and thus enter the TFP gap whereas technical efficiency is rather a long-term phenomenon and should therefore enter TFP growth (and thus, not transmit into the output gap).

With exception of the 2001-2003 recession, the other´downturn episodes are characterized by a drop in TFP below trend. While there are other periods with below trend growth, the decline and bounce-back in TFP growth was short-lived in these non-recession periods. The persistent negative output gap observed in the 1980s is also reflected in an increase in the unemployment gap to about 2% in 1983/84. Subsequently, inefficiencies resulting from the labor market seem to be come less relevant for the output gap, including the Great Recession of 2008/9. Only in the COVID-19 episode, substantial underutilization of capacities arises from the labor volume, most likely due to decreases at the intensive margin due to the 'Kurzarbeit' policy.

Our estimate is aligns well with most of the other estimates by the International Monetary Fund (IMF), the Federal Ministry for Economic Affairs and Climate Action (BMWK) and

[17] The estimate displays moderate estimation uncertainty, as displayed in Figure 21 in Appendix F.

the OECD that only begin in 1981 (1991 in case of the OECD estimate). Especially, the depths of the troughs in 2009 and 2020 are well aligned. Morley and Wong (2020) suggests that a well-behaved output gap should positively correlate with future inflation, and negatively correlate with future output growth, signaling a potential trend reversal. To assess these relationships, we calculate the correlations between our output gap estimate and the one-period-ahead quarter-on-quarter growth rates of both GDP and the consumer price index. Our analysis reveals a positive correlation of 0.4 with future GDP growth and a negative correlation of -0.x with inflation for the sample period. These correlation values provide valuable insights into the plausibility and behavior of our output gap estimate, aligning with the expected economic patterns.

Output gap

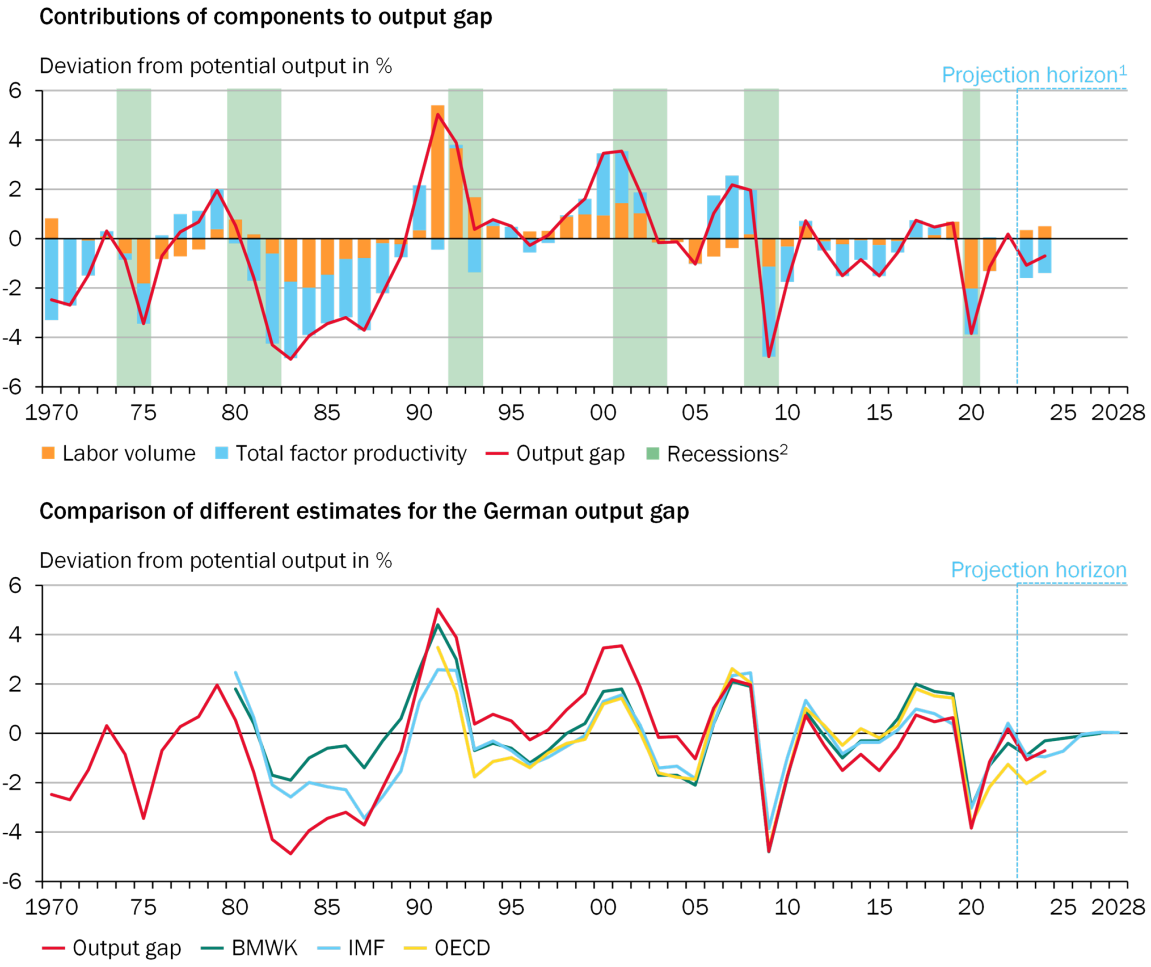

1 – Values for 2023 and 2024 are based on the short-term forecast by the GCEE. 2 – Recessions dated by the GCEE.

Sources: BMWK, Federal Statistical Office, IMF, OECD, own calculations

Figure 19

F Further Distributional Estimates

Figures 20, 21 and 22 depict distributional estimates (5% to 95% quantiles in blue, 50% quantile in black) of potential output growth, the output gap and total factor productivity. Shaded areas indicate the short-run and the long-run forecast horizons, respectively.

Distributional estimate of potential output growth

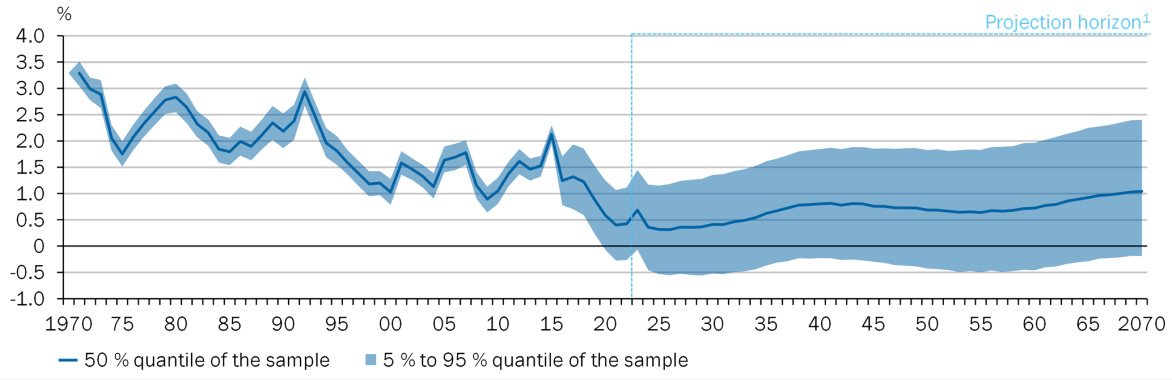

1 – Values for 2023 and 2024 are based on the German Council of Economic Experts' short-term forecast. From 2025 projection, results of the reference scenario.

Sources: Federal Statistical Office, IAB, OECD, own calculations
© Sachverständigenrat | 23-428-01

Figure 20

Distributional estimate of the output gap

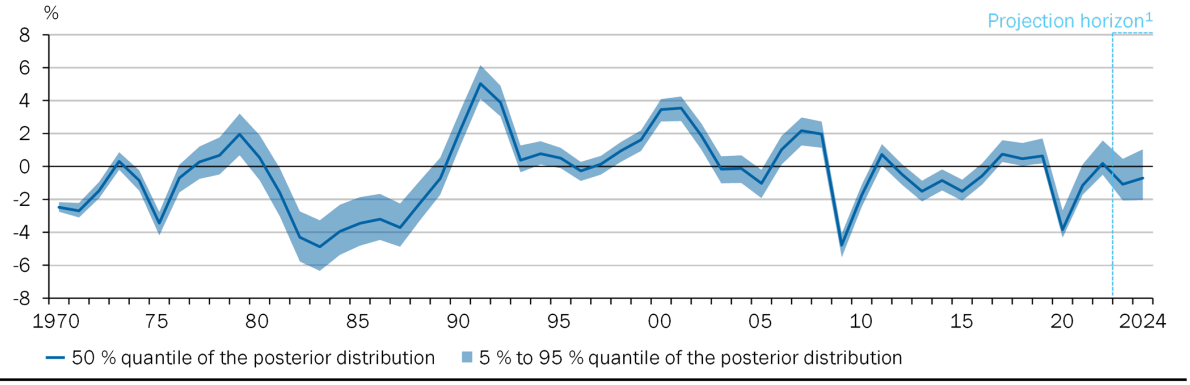

1 – Values for 2023 and 2024 are based on the German Council of Economic Experts' short-term forecast.

Sources: Federal Statistical Office, IAB, OECD, own calculations
© Sachverständigenrat | 23-429-01

Figure 21

Total factor productivity[1]

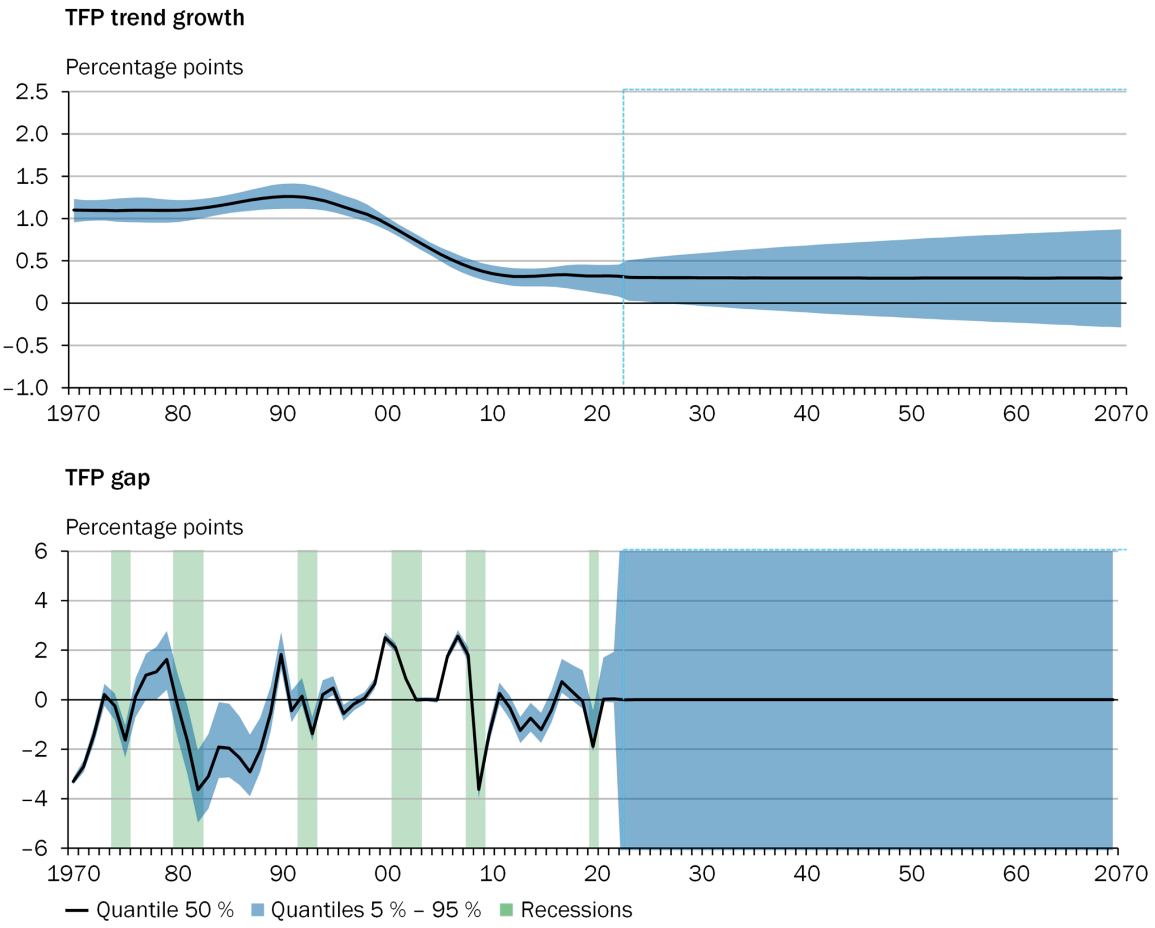

1 – Results are based on 50,000 retained posterior draws. Blue shaded area indicates 90 % probability mass.

Sources: Federal Statistical Office, IAB, OECD, own calculations

Figure 22

G Baseline filter

This Appendix outlines the estimation of the baseline filter. To disentangle persistent and transitory signals, we employ a standard unobserved-component framework. Thus, in this section, trends and cycles do not necessarily have a structural interpretation. Furthermore, note that the notation is specific to this section. To estimate the unobserved components, we rely on a straightforward precision-sampling algorithm in the spirit of Chan and Jeliazkov (2009) or Mertens (2023). A similar model is presented by Chan et al. (2013). All computations are implemented in `R` by using the `btsm` package (**?**).

G.1 Trend-Cycle Specification

Our goal is to decompose observed data x_t into its trend x_t^τ and its cycle x_t^c. The equations are

$$x_t = x_t^\tau + x_t^c \tag{22}$$
$$x_t^\tau = x_{t-1}^\tau + x_t^g + \eta_t^\tau \qquad \eta_t^\tau \sim \mathcal{TN}\left(0, \sigma_\tau^2\right)_{\left[\underline{x_t^\tau} - x_{t-1}^\tau, \overline{x_t^\tau} - x_{t-1}^\tau\right)} \tag{23}$$
$$x_t^g = x_{t-1}^g + \eta_t^g \qquad \eta_t^g \sim \mathcal{N}\left(0, \sigma_g^2\right) \tag{24}$$
$$x_t^c = \phi_t x_{t-1}^c + \eta_t^c \qquad \eta_t^c \sim \mathcal{N}\left(0, \exp\left(\psi_t\right)\right) \tag{25}$$
$$\phi_t = \phi_{t-1} + \eta_t^\phi \qquad \eta_t^\phi \sim \mathcal{TN}\left(0, \sigma^\phi\right)_{[0-\phi_{t-1}, 1-\phi_{t-1})} \tag{26}$$
$$\psi_t = \psi_{t-1} + \eta_t^\psi \qquad \eta_t^\psi \sim \mathcal{N}\left(0, \sigma_\psi^2\right) \tag{27}$$

where $\mathcal{N}$ denotes the normal distribution, $\mathcal{TN}$ denotes the truncated normal distribution, the innovation distribution subscript in Eq. 23 indicates bounded support. The innovations are mutually orthogonal across Eqs. 23 – 27 in all $t = 1 \dots T$ and $\underline{x_t^\tau}$ and $\overline{x_t^\tau}$ are known constants.

To find the prior distributions of all components, a more compact notation is helpful. Stacking the components in Eqs. 22 – 27 over T, we obtain

$$\boldsymbol{x} = \boldsymbol{x}^\tau + \boldsymbol{x}^c \tag{28}$$
$$\boldsymbol{D}_1 \boldsymbol{x}^\tau = (x_0^\tau, \mathbf{0}'_{T-1})' + \boldsymbol{x}^g + \boldsymbol{\eta}^\tau \qquad \boldsymbol{\eta}^\tau \sim \mathcal{TN}\left(\mathbf{0}_T, \boldsymbol{\Sigma}_\tau\right) \tag{29}$$
$$\boldsymbol{D}_1 \boldsymbol{x}^g = (x_0^g, \mathbf{0}'_{T-1})' + \boldsymbol{\eta}^g \qquad \boldsymbol{\eta}^g \sim \mathcal{N}\left(\mathbf{0}_T, \boldsymbol{\Sigma}_g\right) \tag{30}$$
$$\boldsymbol{D}_\phi \boldsymbol{x}^c = \boldsymbol{\eta}^c \qquad \boldsymbol{\eta}^c \sim \mathcal{N}\left((\phi_1(x_0 - x_0^\tau), \mathbf{0}'_{T-1})', exp\left(\boldsymbol{\Psi}\right)\right) \tag{31}$$
$$\boldsymbol{D}_1 \boldsymbol{\phi} = (\phi_0, \mathbf{0}'_{T-1})' + \boldsymbol{\eta}^\phi \qquad \boldsymbol{\eta}^\phi \sim \mathcal{TN}\left(\mathbf{0}_T, \boldsymbol{\Sigma}_\phi\right) \tag{32}$$
$$\boldsymbol{D}_1 \boldsymbol{\psi} = (\psi_0, \mathbf{0}'_{T-1})' + \boldsymbol{\eta}^\psi \qquad \boldsymbol{\eta}^\psi \sim \mathcal{N}\left(\mathbf{0}_T, \boldsymbol{\Sigma}_\psi\right), \tag{33}$$

where bold expressions refer to vectors and matrices and $\mathbf{0}_{T-1}$ is a $T-1 \times 1$ vector of

zeros and

$$\boldsymbol{x}^* = \begin{bmatrix} x_1 \\ x_2 \\ \vdots \\ x_T \end{bmatrix} \qquad \boldsymbol{\eta}^* = \begin{bmatrix} \eta_1 \\ \eta_2 \\ \vdots \\ \eta_T \end{bmatrix} \qquad \boldsymbol{\phi} = \begin{bmatrix} \phi_1 \\ \phi_2 \\ \vdots \\ \phi_T \end{bmatrix}$$

$$\boldsymbol{D}_1 = \begin{bmatrix} 1 & & & & \\ -1 & 1 & & & \\ & -1 & 1 & & \\ & & \ddots & \ddots & \\ & & & -1 & 1 \end{bmatrix} \qquad \boldsymbol{D}_\phi = \begin{bmatrix} 1 & & & & \\ -\phi_2 & 1 & & & \\ & -\phi_3 & 1 & & \\ & & \ddots & \ddots & \\ & & & -\phi_T & 1 \end{bmatrix}$$

$$\boldsymbol{\Sigma}_* = \begin{bmatrix} \sigma_*^2 & & & & \\ & \sigma_*^2 & & & \\ & & \sigma_*^2 & & \\ & & & \ddots & \\ & & & & \sigma_*^2 \end{bmatrix} \qquad \boldsymbol{\Psi} = \begin{bmatrix} \psi_1 & & & & \\ & \psi_2 & & & \\ & & \psi_4 & & \\ & & & \ddots & \\ & & & & \psi_T \end{bmatrix}$$

where the non-specified elements are zero and * indexes τ, g, ϕ, ψ and $\boldsymbol{\Sigma}_\phi = diag(\xi_\phi, \sigma_\phi^2 \dots \sigma_\phi^2)$. Our goal is to sample from the joint density $p(\boldsymbol{\theta})$ with $\boldsymbol{\theta} = \left(\boldsymbol{x}^\tau, \boldsymbol{x}^g, \boldsymbol{\phi}, \boldsymbol{\Psi}, \sigma_\tau^2, \sigma_g^2, \sigma_\phi^2, \sigma_\psi^2, x_0^\tau, x_0^g, \phi_0, \psi_0\right)$. We can do so with the help of Gibbs sampling, using precision-based algorithms in the spirit of Chan and Jeliazkov (2009). Given the stacked transition equations (28)-(33), it is straightforward to find explicit expressions for some of the prior distributions, i.e.

$$p(\boldsymbol{x}^\tau) \text{ is } \mathcal{TN}\left(\boldsymbol{D}_1^{-1}(\overline{\boldsymbol{x}}^\tau + \boldsymbol{x}^g),\ \boldsymbol{D}_1^{-1'}\boldsymbol{\Sigma}_\tau\boldsymbol{D}_1^{-1}\right)_{\left[\underline{\boldsymbol{x}^\tau}, \overline{\boldsymbol{x}^\tau}\right)} \tag{34}$$

$$p(\boldsymbol{x}^g) \text{ is } \mathcal{N}\left(\boldsymbol{D}_1^{-1}\overline{\boldsymbol{x}}^g,\ \boldsymbol{D}_1^{-1'}\boldsymbol{\Sigma}_g\boldsymbol{D}_1^{-1}\right) \tag{35}$$

$$p(\boldsymbol{x}^c) \text{ is } \mathcal{N}\left((\phi_1(x_0 - x_0^\tau), \mathbf{0}'_{T-1})',\ \boldsymbol{D}_\phi^{-1'}\boldsymbol{\Psi}\boldsymbol{D}_\phi^{-1}\right) \tag{36}$$

$$p(\boldsymbol{\phi}) \text{ is } \mathcal{TN}\left(\boldsymbol{D}_\mathbf{1}^{-1}\overline{\boldsymbol{\phi}}_c,\ \boldsymbol{D}_1^{-1'}\boldsymbol{\Sigma}_\phi\boldsymbol{D}_1^{-1}\right)_{[0,1)} \tag{37}$$

where $\overline{\boldsymbol{x}}^\tau = (x_0^\tau, \mathbf{0}'_{T-1})'$, $\overline{\boldsymbol{x}}^g = (x_0^g, \mathbf{0}'_{T-1})'$, $\overline{\boldsymbol{\phi}}_c = (\phi_0, \mathbf{0}'_{T-1})$ as well as $\overline{\boldsymbol{\psi}} = (\psi_0, \mathbf{0}'_{T-1})$. In addition, we assume normal priors for initial states and we use standard inverse-Gamma

priors with shape a and scale b for the time-constant innovation variances, i.e.

$$p\left(x_0^\tau\right) \text{ is } \mathcal{N}\left(\mu_\tau,\ \xi\tau\right) \tag{38}$$
$$p\left(x_0^g\right) \text{ is } \mathcal{N}\left(\mu_g,\ \xi_g\right) \tag{39}$$
$$p\left(\phi_0\right) \text{ is } \mathcal{N}\left(\mu_\phi,\ \xi_\phi\right) \tag{40}$$
$$p\left(\psi_0\right) \text{ is } \mathcal{N}\left(\mu_\psi,\ \xi_\psi\right) \tag{41}$$
$$p\left(\sigma_\tau^2\right) \text{ is } \mathcal{IG}\left(a_\tau, b_\tau\right) \tag{42}$$
$$p\left(\sigma_g^2\right) \text{ is } \mathcal{IG}\left(a_g, b_g\right) \tag{43}$$
$$p\left(\sigma_\psi^2\right) \text{ is } \mathcal{IG}\left(a_\psi, b_\psi\right) \tag{44}$$
$$p\left(\sigma_\phi^2\right) \text{ is } \mathcal{IG}\left(a_\phi, b_\phi\right). \tag{45}$$

G.2 Conditional Distributions of the Trend and Trend Growth

To find the posterior distributions, we need to specify the log conditional likelihoods. Let $\boldsymbol{\theta}^-$ denote the vector of all parameters that are conditioned upon. For Eq. 22, the log conditional likelihood obtains as

$$\begin{aligned}\log p\left(\boldsymbol{x}|\boldsymbol{\theta}^-\right) \propto &-\frac{1}{2}\sum_{t=1}^{T}\psi_t - \frac{1}{2}(\boldsymbol{x} - \boldsymbol{D}_\phi^{-1}\mathbb{E}(\boldsymbol{x}^c) - \boldsymbol{x}^\tau)' \\ &\times \boldsymbol{D}_\phi'\boldsymbol{\Sigma}_c^{-1}\boldsymbol{D}_\phi(\boldsymbol{x} - \boldsymbol{D}_\phi^{-1}\mathbb{E}(\boldsymbol{x}^c) - \boldsymbol{x}^\tau)\end{aligned} \tag{46}$$

where $\boldsymbol{\Sigma}_c = \exp(\boldsymbol{\Psi})^{-1}$, $\mathbb{E}(\boldsymbol{x}^c) = (\phi_1(x_0 - x_0^\tau), \mathbf{0}_{T-1}')'$, and $\widetilde{\mathcal{N}}$ is the standard normal cumulative distribution function, such that the conditional posterior of $\boldsymbol{x}^\tau$ follows as

$$p\left(\boldsymbol{x}^\tau|\boldsymbol{\theta}^-\right) \text{ is } \mathcal{TN}\left(\boldsymbol{\Omega}_\tau^{-1}(\boldsymbol{D}_1\boldsymbol{\Sigma}_\tau^{-1}(\overline{\boldsymbol{x}}^\tau + \boldsymbol{x}^g) + \boldsymbol{D}_\phi'\boldsymbol{\Sigma}_c^{-1}\boldsymbol{D}_\phi(\boldsymbol{x} - \boldsymbol{D}_\phi^{-1}\mathbb{E}(\boldsymbol{x}^c))), \boldsymbol{\Omega}_\tau^{-1}\right)_{\left[\underline{\boldsymbol{x}^\tau}, \overline{\boldsymbol{x}^\tau}\right)} \tag{47}$$

with $\boldsymbol{\Omega}_\tau = \boldsymbol{D}_1\boldsymbol{\Sigma}_\tau^{-1}\boldsymbol{D}_1 + \boldsymbol{D}_\phi'\boldsymbol{\Sigma}_c^{-1}\boldsymbol{D}_\phi$. Then,

$$\boldsymbol{x}^c = \boldsymbol{x} - \boldsymbol{x}^\tau. \tag{48}$$

To sample $\boldsymbol{x}^g$, note that the log conditional likelihood of $\boldsymbol{D}_1(\boldsymbol{x}^\tau - \boldsymbol{D}_1\overline{\boldsymbol{x}}^\tau)$ is proportional to

$$-\frac{1}{2}(\boldsymbol{D}_1(\boldsymbol{x}^\tau - \boldsymbol{D}_1\overline{\boldsymbol{x}}^\tau) - \boldsymbol{x}^g)'\boldsymbol{\Sigma}_\tau^{-1}(\boldsymbol{D}_1(\boldsymbol{x}^\tau - \boldsymbol{D}_1\overline{\boldsymbol{x}}^\tau) - \boldsymbol{x}^g), \tag{49}$$

such that we find that

$$p\left(\boldsymbol{x}^g|\boldsymbol{\theta}^-\right) \text{ is } \mathcal{N}\left(\boldsymbol{\Omega}_g^{-1}(\boldsymbol{D}_1'\boldsymbol{\Sigma}_\tau^{-1}\overline{\boldsymbol{x}}^g + \boldsymbol{D}_1'\boldsymbol{\Sigma}_g^{-1}\boldsymbol{D}_1(\boldsymbol{D}_1(\boldsymbol{x}^\tau - \boldsymbol{D}_1\overline{\boldsymbol{x}}^\tau))), \boldsymbol{\Omega}_g^{-1}\right) \tag{50}$$

with $\boldsymbol{\Omega}_g = \boldsymbol{\Sigma}_\tau^{-1} + \boldsymbol{D}_1'\boldsymbol{\Sigma}_g^{-1}\boldsymbol{D}_1$.

G.3 Conditional Distribution of the Stochastic Volatility

To estimate the stochastic volatilities of $\boldsymbol{x}^c$, we use the auxiliary mixture sampler of Kim et al. (1998). That is, we compute $\widetilde{\boldsymbol{x}^c} = \log\left((\boldsymbol{D}_\phi\boldsymbol{x}^c)^2\right)$ and approximate the log-normal innovations by means of a seven-point-normal-mixture distribution. Let $\widetilde{\eta}^c \sim \mathcal{N}(\boldsymbol{\mu}_m, \boldsymbol{\Sigma}_m)$

denote the log-normal mixture distribution conditional on the mixture indicators. The log conditional likelihood of $\widetilde{\boldsymbol{x}^c}$ is proportional to

$$-\frac{1}{2}(\widetilde{\boldsymbol{x}^c} - \boldsymbol{\psi} - \boldsymbol{\mu}_m)'\boldsymbol{\Sigma}_m(\widetilde{\boldsymbol{x}^c} - \boldsymbol{\psi} - \boldsymbol{\mu}_m) \tag{51}$$

In conjunction with the prior of the stochastic volatilities, we find that

$$p\left(\boldsymbol{\psi}|\boldsymbol{\theta}^-\right) \text{ is } \mathcal{N}\left(\boldsymbol{\Omega}_\psi^{-1}\left(\boldsymbol{D}_1'\boldsymbol{\Sigma}_\psi^{-1}\overline{\boldsymbol{\psi}}^c + \boldsymbol{\Sigma}_m^{-1}(\widetilde{\boldsymbol{x}^c} - \boldsymbol{\mu}_m)\right), \boldsymbol{\Omega}_\phi^{-1}\right)_{[0.1)} \tag{52}$$

with $\boldsymbol{\Omega}_\phi = \boldsymbol{\Sigma}_m^{-1} + \boldsymbol{D}_1'\boldsymbol{\Sigma}_\psi^{-1}\boldsymbol{D}_1$.

G.4 Conditional Distribution of the Time-Varying AR(1) Parameter

Define $\boldsymbol{x}_\phi^c$ as a matrix that has the first lag of $\boldsymbol{x}^c$ on its diagonal. From the conditional log likelihood

$$\frac{1}{2}(\boldsymbol{x}^c - \boldsymbol{x}_\phi^c\boldsymbol{\phi})'\boldsymbol{\Sigma}_c^{-1}(\boldsymbol{x}^c - \boldsymbol{x}_\phi^c\boldsymbol{\phi}) \tag{53}$$

and the corresponding prior for $\boldsymbol{\phi}$, we see that the log conditional posterior of $\boldsymbol{\phi}$ is proportional to

$$-\frac{1}{2}\boldsymbol{\phi}'\boldsymbol{D}_1'\boldsymbol{\Sigma}_\phi^{-1}\boldsymbol{D}_1\boldsymbol{\phi} - \sum_{t=2}^{T}\log\left(\widetilde{\mathcal{N}}\left(\frac{1-\phi_{t-1}}{\sigma_\phi}\right) - \widetilde{\mathcal{N}}\left(\frac{-\phi_{t-1}}{\sigma_\phi}\right)\right). \tag{54}$$

Thus,

$$p\left(\boldsymbol{\phi}|\boldsymbol{\theta}^-\right) \text{ is } \mathcal{TN}\left(\boldsymbol{\Omega}_\phi^{-1}\left(\boldsymbol{D}_1\boldsymbol{\Sigma}_\phi^{-1}\overline{\boldsymbol{\phi}}^c + \boldsymbol{X}_\phi'\boldsymbol{\Sigma}_c^{-1}\boldsymbol{x}^c\right), \boldsymbol{\Omega}_\phi^{-1}\right)_{[0.1)} \tag{55}$$

with $\boldsymbol{\Omega}_\phi = \boldsymbol{D}_1'\boldsymbol{\Sigma}_\phi^{-1}\boldsymbol{D}_1 + \boldsymbol{X}_\phi'\boldsymbol{\Sigma}_c^{-1}\boldsymbol{X}_\phi$. To sample from this distribution, we use the `R` package `TruncatedNormal` (Botev 2017, Belzile 2020).

G.5 Conditional Distributions of the Initial Conditions

To sample the initial conditions x_0^τ (if not calibrated), x_0^g, ϕ_1 and ψ_0, it is useful to note that they appear only in the first equations (i.e. $t = 1$) of the relevant transition equation systems specified above. That is, e.g. for the case of x_0^τ, we have

$$x_1^\tau = x_0^\tau + \eta_1^\tau. \tag{56}$$

Therefore, using similar arguments as above, we can derive that

$$p\left(x_0^\tau|\boldsymbol{\theta}^-\right) \text{ is } \mathcal{N}\left(\boldsymbol{\Omega}_{x_0^\tau}^{-1}\left(\frac{\mu_\psi}{\xi_\psi} + \frac{x_1^\tau}{\sigma_\tau^2}\right), \boldsymbol{\Omega}_{x_0^\tau}^{-1}\right), \tag{57}$$

with $\mathbf{\Omega}_{x_0^\tau} = \dfrac{1}{\xi_\tau} + \dfrac{1}{\sigma_\tau^2}$ and

$$p\left(x_0^g|\boldsymbol{\theta}^-\right) \text{ is } \mathcal{N}\left(\mathbf{\Omega}_{x_0^g}^{-1}\left(\frac{\mu_\psi}{\xi_\psi} + \frac{x_1^g}{\sigma_g^2}\right), \mathbf{\Omega}_{x_0^g}^{-1}\right), \tag{58}$$

with $\mathbf{\Omega}_{x_0^g} = \dfrac{1}{\xi_g} + \dfrac{1}{\sigma_g^2}$ and

$$p\left(\phi_0|\boldsymbol{\theta}^-\right) \text{ is } \mathcal{TN}\left(\mathbf{\Omega}_{\phi_0}^{-1}\left(\frac{\mu_\psi}{\xi_\psi} + \frac{\phi_1}{\sigma_\phi^2}\right), \mathbf{\Omega}_{\phi_0}^{-1}\right)_{I_{[0.1)}}, \tag{59}$$

with $\mathbf{\Omega}_{\phi_0} = \dfrac{1}{\xi_\phi} + \dfrac{1}{\sigma_\phi^2}$ and

$$p\left(\psi_0|\boldsymbol{\theta}^-\right) \text{ is } \mathcal{N}\left(\mathbf{\Omega}_{\psi_0}^{-1}\left(\frac{\mu_\psi}{\xi_\psi} + \frac{\psi_1}{\sigma_\psi^2}\right), \mathbf{\Omega}_{\psi_0}^{-1}\right), \tag{60}$$

with $\mathbf{\Omega}_{\psi_0} = \dfrac{1}{\xi_\psi} + \dfrac{1}{\sigma_\psi^2}$.

G.6 Conditional Distributions of the Innovation Variances

Similarly, in the spirit of the previous arguments, it can be shown that

$$p\left(\sigma_\tau^2|\boldsymbol{\theta}^-\right) \text{ is } \mathcal{IG}\left(a_\tau + \frac{T}{2},\ b_\tau + \frac{1}{2}(\boldsymbol{x}^\tau - x_0^\tau \mathbf{1}_T)'\boldsymbol{D}_1'\boldsymbol{D}_1(x^\tau - x_0^\tau \mathbf{1}_T)\right) \tag{61}$$

$$p\left(\sigma_g^2|\boldsymbol{\theta}^-\right) \text{ is } \mathcal{IG}\left(a_g + \frac{T}{2},\ b_g + \frac{1}{2}(\boldsymbol{x}^g - x_0^g \mathbf{1}_T)'\boldsymbol{D}_1'\boldsymbol{D}_1(\boldsymbol{x}^g - x_0^g \mathbf{1}_T)\right) \tag{62}$$

$$p\left(\sigma_\psi^2|\boldsymbol{\theta}^-\right) \text{ is } \mathcal{IG}\left(a_\psi + \frac{T}{2},\ b_\psi + \frac{1}{2}\left(\boldsymbol{\psi} - \psi_0 \mathbf{1}_T\right)'\boldsymbol{D}_1'\boldsymbol{D}_1\left(\boldsymbol{\psi} - \psi_0 \mathbf{1}_T\right)\right) \tag{63}$$

$$p\left(\sigma_\phi^2|\boldsymbol{\theta}^-\right) \text{ is } \mathcal{IG}\left(a_\phi + \frac{T}{2},\ b_\phi + \frac{1}{2}\left(\boldsymbol{\phi} - \phi_0 \mathbf{1}_T\right)'\boldsymbol{D}_1'\boldsymbol{D}_1\left(\boldsymbol{\phi} - \phi_0 \mathbf{1}_T\right)\right) \tag{64}$$

where $\mathbf{1}_T$ is the $T \times 1$ unit vector.

G.7 Gibbs Sampler

The estimation routine then involves iterating through the following steps, conditional on the previous draws (the draw index is suppressed for convenience):

Block 1

1. Draw $\boldsymbol{x}^\tau$ from Eq. 47.
2. Draw x_0^τ from Eq. 57.
3. Draw σ_τ^2 from Eq. 61.

Block 2

4. Draw $\boldsymbol{x}^g$ from Eq. 50.
5. Draw x_0^g from Eq. 58.
6. Draw σ_g^2 from Eq. 62.

Block 3

7. Compute $\boldsymbol{x}^c$ with the help of Eq. 48.
8. Draw $\boldsymbol{\phi}$ from Eq. 55.
9. Draw ϕ_0 from Eq. 59.
10. Draw σ_ϕ^2 from Eq. 64.

Block 4

11. Draw ψ from Eq. 52.
12. Draw ψ_0 from Eq. 60.
13. Draw σ_ψ^2 from Eq. 63.

In our analysis, we generated a total of 360,000 samples from the conditional posterior distribution. To ensure the reliability of our results, we discarded the initial 10,000 samples as they can be less representative of the true distribution. To enhance the quality of our samples, we only kept every seventh sample, which helps improve the overall mixing and efficiency of our estimation process.

To predict future values from our model, we rely on the posterior distribution of the model's parameters and latent states. This predictive distribution is constructed by simulating new innovations and then iterating the state equations. We carried out this simulation process using the R programming language, leveraging the capabilities of the `btsm` package, as outlined in Ochsner (forthcoming).

H Random Walk Model

In certain situations, our objective is to estimate the parameters of a process denoted as x_t^τ, which does not exhibit cyclical variations. The equations governing this process are as follows:

$$x_t^\tau = x_{t-1}^\tau + x_t^g + \eta_t^\tau \qquad \eta_t^\tau \sim \mathcal{N}\left(0, \sigma_\tau^2\right) \tag{65}$$

$$x_t^g = x_{t-1}^g + \eta_t^g \qquad \eta_t^g \sim \mathcal{N}\left(0, \sigma_g^2\right), \tag{66}$$

where the definitions from Appendix G apply.

We aim to determine the prior distributions of the various components of this process. To simplify the notation, we stack these equations over the time period T, resulting in the following representations:

$$\boldsymbol{D}_1 \boldsymbol{x}^\tau = \boldsymbol{x}^g + \boldsymbol{\eta}^\tau \qquad \boldsymbol{\eta}^\tau \sim \mathcal{N}\left(\mathbf{0}_T, \boldsymbol{\Sigma}_\tau\right) \tag{67}$$

$$\boldsymbol{D}_1 \boldsymbol{x}^g = \boldsymbol{\eta}^g \qquad \boldsymbol{\eta}^g \sim \mathcal{N}\left(\mathbf{0}_T, \boldsymbol{\Sigma}_g\right), \tag{68}$$

where again the definitions from Appendix G apply. Notably, the model presented in a previous section nests these equations, which means that the same computational algorithms can be applied using the R programming language and the `btsm` package.